The transcriptional co-regulators NBCL1 and NBCL2 redundantly coordinate aerial organ development and root nodule identity in legumes

Shengbin Liu, Kévin Magne, Jing Zhou, Juliette Laude, Marion Dalmais, Christine Le Signor, Abdelhafid Bendahmane, Richard Thompson, Jean-Malo Couzigou, Pascal Ratet

The transcriptional co-regulators NBCL1 and NBCL2 redundantly coordinate aerial organ development and root nodule identity in legumes

Shengbin Liu[1,2], Kévin Magne[1,2,a], Jing Zhou[3], Juliette Laude[1,2], Marion Dalmais[1,2], Christine Le Signor[4], Abdelhafid Bendahmane[1,2], Richard Thompson[4], Jean-Malo Couzigou[3] and Pascal Ratet[1,2,a]

[1] Université Paris-Saclay, CNRS, INRAE, Univ Evry, Institute of Plant Sciences Paris-Saclay (IPS2), 91190, Gif sur Yvette, France.

[2] Université de Paris, Institute of Plant Sciences Paris-Saclay (IPS2), 91190, Gif sur Yvette, France.

[3] Laboratoire de Recherche en Sciences Végétales, Université de Toulouse, CNRS, UPS, Toulouse INP, 31320, Auzeville Tolosane, France.

[4] Agroécologie, AgroSup Dijon, Institut National de la Recherche Agronomique (INRAE), Université Bourgogne Franche-Comté, 21000, Dijon, France.

[a] Denote corresponding author e-mails: pascal.ratet@cnrs.fr & kevin_magne@hotmail.fr

One sentence summary:

NBCLs coordinate development in legumes

ORCIDs:

(SL): 0000-0001-7512-4225; (KM): 0000-0002-6779-5683; (JMC): 0000-0002-1362-6286; (JZ): 0000-0002-1762-6179; (JL): 0000-0001-7363-1194; (MD): 0000-0002-1673-3095; (CLS): 0000-0002-3204-3537; (AB): 0000-0003-3246-868X; (RT): NONE; (PR): 0000-0002-8621-1495

Abstract

Medicago truncatula NODULE ROOT1 (*MtNOOT1*) and *Pisum sativum COCHLEATA1 (PsCOCH1)* are orthologous genes belonging to the *NOOT-BOP-COCH-LIKE* (*NBCL*) gene family which encodes key transcriptional co-regulators of plant development. In *Mtnoot1* and *Pscoch1* mutants, the development of stipule, flower and symbiotic nodules is altered. *MtNOOT2* and *PsCOCH2* represent the single paralogs of *MtNOOT1* and *PsCOCH1*, respectively. In *M. truncatula*, *MtNOOT1* and *MtNOOT2* are both required for the establishment and maintenance of the symbiotic nodule identity.

In contrast to the *NBCL1* genes, the role of *NBCL2* genes in legume above-ground development is not known. To better understand the roles of *NBCL* genes in legumes, we used *M. truncatula* and *P. sativum nbcl* mutants from the literature, isolated a knockout mutant for the *PsCOCH2* locus and generated *Pscoch1coch2* double mutants in *P. sativum*. These new mutant lines enabled to compare the roles of *MtNOOT2* and *PsCOCH2* in both *M. truncatula* and *P. sativum* legume development.

Our work shows that the single *Mtnoot2* and *Pscoch2* mutants develop wild-type stipules, flowers and symbiotic nodules. However, the number of flowers was increased and the pods and seeds were smaller in comparison to wild type. Furthermore, in comparison to the corresponding *nbcl1* single mutants, both the *M. truncatula* and *P. sativum nbcl* double mutants show a drastic alteration in stipule, inflorescence, flower and nodule development. Remarkably, in both *M. truncatula* and *P. sativum nbcl* double mutants, stipules are transformed into a range of aberrant leaf-like structures.

Key words:

NOOT-BOP-COCH-LIKE, *NODULE-ROOT*, *COCHLEATA*, stipule, inflorescence, development, boundaries, organ identity, symbiosis, *Pisum sativum*, *Medicago truncatula*

Introduction

The *NON-EXPRESSOR OF PATHOGENESIS-RELATED PROTEIN1-LIKE* (*NPR1-LIKE*) genes family encodes transcriptional co-regulators containing BTB/POZ (BROAD COMPLEX, TRAMTRACK and BRICK A BRACK/POXVIRUSES and ZINC FINGER) and ANKYRIN repeat domains (Dong, 2004; Hepworth et al., 2005; Norberg et al., 2005). In particular, the NPR1-LIKE proteins interact with TGACG-type basic leucine zipper (TGA bZIP) to promote the expression of a specific set of genes (Canet et al., 2012, Wang et al., 2019). They can also act as substrate adaptors in E3 ubiquitin ligase complex to regulate PHYTOCHROME INTERACTING FACTOR 4 or LEAFY abundance (Ding et al., 2016; Zhang et al., 2017, Chahtane et al. 2018). This family can be divided into the *NPR1-LIKE* and the *NOOT-BOP-COCH-LIKE* (*NBCL*) subclades which are associated with the regulation of immunity and with the regulation of plant development, respectively (Couzigou et al., 2012). However, cross talks may exist between NBCL and NPR1-LIKE, in particular at the level of TGA bZIP gene induction (Canet et al., 2012). The *NBCL* clade contains the *Medicago truncatula* (*M. truncatula*) *MtNODULE-ROOT1* and *MtNODULE-ROOT2* (*MtNOOT1* and *2*) genes, the *Arabidopsis thaliana* (*A. thaliana*) *AtBLADE-ON-PETIOLE1* and *AtBLADE-ON-PETIOLE 2* (*AtBOP1* and *2*) genes, and the *Pisum sativum* (*P. sativum*) *PsCOCHLEATA1* and *PsCOCHLEATA2* (*PsCOCH1* and *2*) genes (Couzigou et al., 2012).

The *A. thaliana AtBOP1* and *AtBOP2* genes represent the founders and best-characterized *NBCL* genes. AtBOP1/2 have a dual function, repressing genes that confer meristem cell fate and inducing genes that promote lateral organ fate and polarity in aerial organs (Ha et al., 2007). AtBOP1/2 are required for the production of various determinate lateral organs including stipules, nectaries and flowers in eudicots (reviewed in Khan et al., 2014; Hepworth and Pautot, 2015; Wang et al., 2016). The *AtBOP1* and *AtBOP2* genes play important roles in regulating leaf morphogenesis and patterning along the proximo-distal axis (Ha et al., 2003; Ha et al., 2007). The *bop1-1* dominant-negative and *bop1bop2* double mutant leaves form ectopic blade tissues along cotyledons and along leaf petioles (Ha et al., 2003). In developing leaf primordia, AtBOP1 and AtBOP2 negatively regulate the expression of the class I *KNOX* genes *BREVIPEDICELLUS* (*AtBP*), *KNOTTED-LIKE FROM ARABIDOPSIS THALIANA 2* (*KNAT2*), and *KNOTTED-LIKE FROM ARABIDOPSIS THALIANA 6* (*KNAT6*; Ha et al., 2003; Hepworth et al., 2005; Norberg et al., 2005; Ha et al., 2007). During *A. thaliana* reproductive development, AtBOP1 and AtBOP2 redundantly control floral patterning, floral organ number, bract suppression, gynoecium formation and inflorescence architecture (Ha et al., 2003;

Norberg et al., 2005; Ha et al., 2007; Xu et al., 2010; Khan et al. 2012b, Hepworth and Pautot, 2015).

NBCL activities in *A. thaliana*, *Nicotiana tabacum*, *M. truncatula*, *L. japonicus*, *P. sativum* and *Lupinus angustifolius* are essential for the differentiation of abscission zones of leaflets, petioles, petals and fruit, which is a prerequisite for organ abscission (Hepworth et al., 2005; Norberg et al., 2005; McKim et al., 2008; Wu et al., 2012; Couzigou et al. 2016; Xu et al., 2016).

In *Solanum lycoperscum*, three BLADE-ON-PETIOLE paralogs (SlBOP1, 2 and 3) also control inflorescence architecture (Xu et al., 2016; Izhaki et al., 2018) and compound leaf complexity (Ichihashi et al., 2014). This regulation of inflorescence architecture by NBCLs is also observed in several monocot species such as *Brachypodium distachyon*, *Oryza sativa*, *Hordeum vulgare* and *Zea mays* (Tavakol et al., 2015; Jost et al., 2016; Dong et al., 2017; Toriba et al., 2019; Magne et al., 2020).

In the grasses *H. vulgare*, *O. sativa* and *B. distachyon*, the *NBCL* genes are also required for the patterning of the leaf, especially for the patterning of the ligular region (Tavakol et al., 2015; Toriba et al., 2019; Magne et al., 2020; Liu et al., 2021). In *O. sativa*, the *OsBOP* genes determine the leaf sheath-blade ratio through the activation of proximal sheath differentiation and suppression of distal blade differentiation (Toriba et al., 2019). Altogether, these studies showed that various biological processes, such as leaf development, floral patterning, inflorescence architecture or abscission zone development, are regulated by NBCLs even in distant eudicots and grasses species, arguing for the inheritance of ancestral functions rather than for a converging mechanism. Interestingly enough, the conserved regulation of many developmental processes, the retention and functional redundancy between paralogs after whole genome duplication are hallmark features of NBCLs. However, the relative importance of each NBCL copy in the regulation of various biological processes varies across species and processes, thus it represents a nice framework to study the mechanisms of gene conservation, sub-functionalization, neo-functionalization or specialization in evo-devo (Assis and Bachtrog, 2013).

The study of *NBCL* in legumes originated from the discovery of the *P. sativum Pscochleata1* (*Pscoch1*) mutant affected for stipule development (Wellensiek, 1959; Blixt, 1967). Later, the corresponding gene *PsCOCH1* was also shown to be required for the development of *P. sativum* inflorescence, flower and for symbiotic nodule identity maintenance (Yaxley et al., 2001; Ferguson and Reid, 2005; Couzigou et al., 2012; Sharma et al., 2012). Fifty years after the first mention of the *cochleata* mutation in the literature and its extensive

use as a morphological genetic marker, we discovered that *M. truncatula MtNOOT1* and *P. sativum PsCOCH1* were orthologous to the *A. thaliana AtBOP* genes (Zhukov et al., 2007; Couzigou et al., 2012). Furthermore, we also showed that paralogs of *MtNOOT1* and *PsCOCH1*, namely *MtNOOT2* and *PsCOCH2*, exist in *M. truncatula* and *P. sativum*, respectively (Magne et al., 2018a).

In agreement with the *Pscoch1* phenotypes, the *M. truncatula Mtnoot1* mutants have simplified stipules with a number of digitations remaining low throughout the development of the plant (Couzigou et al., 2012). In the *Mtnoot1* mutants, flowers show additional floral organs and suggest a reduced penetrance of the *nbcl1* mutation in *M. truncatula* compared to *P. sativum* (Couzigou et al., 2012). In *Lotus japonicus* (*L. japonicus*), there is a single *NBCL* copy called *LjNBCL1* that controls the development of leaves, nectaries and flowers (Magne et al., 2018b). The presence of a single *NBCL* copy in *L. japonicus* seems to be a specific case in Papilionoids and, in comparison with the *Pscoch1* and the *Mtnoot1* phenotypes, the stronger *Ljnbcl1* phenotype suggests that the two legume *NBCL* genes (*NBCL1* and *NBCL2*) control different aspects of development.

To better understand the specific and redundant roles of legume *NBCL1* and *NBCL2* genes in development and NBCLs sub-functionalization during legume evolution, we applied reverse genetic approaches in the model legume species *M. truncatula* and *P. sativum*. We hypothesized that the mild phenotypes observed in *Mtnoot1* mutant when compared to *Pscoch1* could be explained by functional redundancy of legume *NBCLs* and an imbalanced functional weight of *NBCL1* and *NBCL2* between *M. truncatula* and *P. sativum*. In this study, we isolated a null allele for *PsCOCH2* locus and generated *Pscoch1coch2* double mutants. We then compared the phenotypes of the *P. sativum* and *M. truncatula nbcl1* and *nbcl2* single mutants, as well as those of the *nbcl1nbcl2* double mutants.

Our work shows that the *Mtnoot2* and *Pscoch2* mutants are not affected in stipules, leaves or flowers development but that seeds were smaller. In contrast, in *Mtnoot1noot2* and *Pscoch1coch2*, stipules and flowers were strongly modified and these phenotypes were increased in comparison to the corresponding *nbcl1* single mutants. Our results suggest that in legumes, together with NBCL1, NBCL2 contributes to vegetative and reproductive development.

Moreover, similarly to what was described in *M. truncatula* (Magne et al., 2018a), the *Pscoch2* single mutant was not altered for symbiotic nodule development nor for nodule identity maintenance. However, *Pscoch1coch2* nodules were smaller, supernumerary and

showed a high level of nodule-to-root conversion events associated with a reduced nitrogen fixation efficiency.

Our findings show that the legume specific *NBCL2* genes play important roles in the development of various organs such as stipules, flowers, seeds and indeterminate nodules.

MATERIALS AND METHODS

Plant material

For *M. truncatula* studies, we used the wild type *M. truncatula* ecotype R-108 (Hoffmann et al., 1997). The corresponding *Mtnoot1*, *Mtnoot2* and *Mtnoot1Mtnoot2* mutants are described in the **Fig. 1** of this manuscript as well as in Couzigou et al., 2012 and Magne et al., 2018a. The transgenic line R-108::*PromNOOT2*:GUS is described in Magne et al., 2018a.

For *P. sativum* studies, we used the wild type *P. sativum* var. Caméor, var. JI2822 and var. SGE. The corresponding *Pscoch1*, *Pscoch2* and *Pscoch1coch2* mutants are described in the **Fig. 1** of this manuscript as well as in Zhukov et al. 2007 and Couzigou et al., 2012.

P. sativum var. Caméor *Pscoch2* TILLING mutant screen.

The *P. sativum* var. Caméor ethylmethane sulfonate (EMS) TILLING collection represents 4817 individual M2 families (Dalmais et al., 2008; http://urgv.evry.inra.fr/UTILLdb). This collection is available at the legume centre for genetic resources at the UMR1347 of Dijon, Institut National de Recherche pour l'Agriculture, l'Alimentation et l'Environnement (INRAE) and was screened by TILLING-NGS technology for putative point mutations in the *PsCOCHLEATA2* genes (KX821778, KX821779, KX821780, KX821781) at the Unité de Recherche en Génomique Végétales (INRAE). Oligonucleotides sequences used for both TILLING-NGS screen and genotyping are given in **Supplementary Table S5**.

Plant growth conditions

For vegetative development and bloom, *M. truncatula* and *P. sativum* seeds were scarified with sand paper and surface-sterilized in 20 mL of sodium hypochlorite (one pellet per 1 L of sterile water) and 1 droplet of liquid soap during 20 min under agitation. Three successive washes were performed with sterile water. Seeds were stratified for 2 days at 4°C under darkness on 7 $g.L^{-1}$ Kalys Agar plates. Seeds were then transferred to growth chamber 48 h at 24°C under darkness for acclimatization. Seedlings were grown in a loam/peat/sand mixture (70/3,5/7, v/v/v; http://www.puteaux-sa.fr) with expensed clay balls at the bottom of the pot. Plants were grown in greenhouses under 16/8-h light/dark cycle, 24°C/24°C day/night temperature, relative humidity of 60% and 200 µE of light intensity). Plants were watered with N+ nutritive solution (Soluplant, NPK:16-6-26; https://www.haifa-group.com/fr/soluplant).

For *P. sativum* nodulation assays, seedlings were transferred in pots containing a sand/perlite mixture (1/2, v/v) and inoculated with 25 mL of *Rhizobium leguminosarum* bv. *viciae* wild type strain P221 at $OD_{600\ nm}$: 0,1 (Laguerre et al., 1992). Rhizobia were grown on Yeast Extract Mannitol (YEM; Bergersen, 1961; Na_2HPO_4, 460 $mg.L^{-1}$; $MgSO_4$, 100 $mg.L^{-1}$; $FeCl_3$, 4 $mg.L^{-1}$; $CaCl_2$, 40 $mg.L^{-1}$; sodium hydrogeno glutamate, 1.1 $g.L^{-1}$; mannitol 10 $g.L^{-1}$; yeast extract, 200 $mg.L^{-1}$; bacto agar, 15 $g.L^{-1}$; pH: 6,8) for 2 days under darkness at 28°C. Inoculated plants were grown in a growth chamber under 16/8h light-dark cycle, 24/24°C day-night temperature, 60% of relative humidity and 200 µE of light intensity. Plants were watered three times a week (2 times with tap water and 1 time with HY N-free nutritive solution). For 5 liters of HY N-free solution: 50 mL of stock solutions (KH_2PO_4, 0,1 M; $MgSO_4$, 0,1 M); 12,5 mL of stock solutions (K_2SO_4, 0,1 M; $CaCl_2$, $2H_2O$, 0,1 M); 5 mL of stock solutions (KCl, 50 mM; H_3BO_3, 23,8 mM; MnSO4, H_20, 5 mM; $ZnSO_4$, $7H_20$, 1 mM; $CuSO_4$, 1 mM; $MoNa_2O_4$, $2H_20$, 0,7 mM; Na-Fe-EDTA, 98 mM); pH: 7).

M. truncatula and *P. sativum* DNA extraction and genotyping

M. truncatula and *P. sativum* genomic DNA were extracted from young leaves using phenol-chloroform and CTAB procedures, respectively. *M. truncatula Tnt1* mutants were genotyped by PCR as described in Magne et al., 2018a. *P. sativum* TILLING point mutations were genotyped by PCR and sequencing. PCR amplifications were carried out using High Fidelity Taq DNA polymerase (EUROBIO GAETHF004D). Information concerning oligonucleotide couples used for PCR are provided in **Supplementary Table S5**. PCR products were sequenced by Sanger (www.eurofinsgenomics.eu) and analyzed with A plasmid Editor 2.0.49 software. For *Pscoch1* FN3185/1325 full-length deletion, deletion borders are unknown and homozygous mutants were selected based on the *Pscoch1* phenotypes.

Gene expression analyses

Total RNA extractions were performed using TRIzol® reagent (Ambion) as described in Magne et al., 2018a. *P. sativum* and *M. truncatula* relative transcripts accumulations were normalized using *PsACTIN* and *PsBETA-TUBULIN3*, and *MtACTIN* and *MtRRM*, respectively. Detailed information concerning oligonucleotides used for RT-qPCR analysis are provided in the **Supplementary Table S6**.

Acetylene reduction assay

Acetylene reduction assays were performed as described in Magne et al., 2018a.

Results

P. sativum and *M. truncatula nbcl* mutants description and *NBCL* genes expression in aerial organs

In *P. sativum*, *M. truncatula* and *L. japonicus*, the *NBCL1* gene functions are conserved for the development of stipules, flowers and nodules (Yaxley et al., 2001; Ferguson and Reid, 2005; Kumar et al., 2009; Kumar et al., 2011; Sinjushin et al., 2011; Couzigou et al., 2012; Sharma et al., 2012; Magne et al., 2018a, 2018b). We also previously identified and characterized the *MtNOOT1* paralog, *MtNOOT2*, in *M. truncatula* and showed the importance of these two *NBCL* paralogs for the symbiotic organ development by using *Mtnoot1* and *Mtnoot2* single mutants as well as *Mtnoot1noot2* double mutants (Couzigou et al., 2012; Magne et al., 2018a).

To further study the roles of *NBCL* paralogs in legume development, we used the *M. truncatula Mtnoot1*, *Mtnoot2* and *Mtnoot1noot2* mutants described above as well as available *P. sativum Pscoch1* mutant alleles described in the literature (Zhukov et al. 2007; Couzigou et al., 2012; **Fig. 1**). In this study, we also looked for null alleles for the *P. sativum PsCOCH2* gene by Targeted Induced Local Lesions IN Genomes coupled with Next Generation Sequencing (TILLING-NGS) in a *P. sativum* var. Caméor TILLING mutant collection (Dalmais et al., 2008). Briefly, 99% of the *PsCOCH2* coding sequence was screened by TILLING-NGS and 75 TILLING mutants were identified. A summary of the TILLING results and the detailed list of the *Pscoch2* TILLING mutants isolated are given in **Supplementary Table S1 and Table S2.** We succeeded in isolating a null allele for the *PsCOCH2* gene of *P. sativum* (*Ps1178*; W122*; **Fig. 1**). Self-fertilized progeny of two heterozygous lines for the *PsCOCH2* locus showed that *PsCOCH2* segregated following the Mendelian Law (**Supplementary Table S3)**. We next constructed *Pscoch1coch2* double mutants by crossing the *Pscoch2 Ps1178* KO mutant with a *Pscoch1*^{JI} FN3185/1325 full-length deletion mutant from the JI2822 background (a progeny line obtained from JI399 CENNIA and JI15 WBH1458 which is genetically close to Caméor, Ellis, T.H.N, personal communication; Jing et al., 2010; **Fig. 1**). The self-fertilized progenies of seven independent F1 heterozygous lines for both the *PsCOCH1* and the *PsCOCH2* locus revealed that *PsCOCH1* and *PsCOCH2* locus segregated as two independent monogenic recessive loci and followed a Mendelian bi-allelic distribution of 9:3:3:1 in the F2 generation (**Supplementary Table S4**).

We first analyzed the expression of *M. truncatula NBCL* genes in the wild type R-108, *Mtnoot1*, *Mtnoot2* and *Mtnoot1noot2* mutant backgrounds. In R-108, both paralogs were expressed in internodes, nodes, leaves, flowers and shoot apical meristem with *MtNOOT1*

generally expressed at a higher level than *MtNOOT2* (**Supplementary Fig. S1A**). *MtNOOT1* and *MtNOOT2* expressions were significantly reduced in their corresponding mutant backgrounds (**Supplementary Fig. S1 D-G**). This analysis showed that inactivation of one paralog did not result in a massive upregulation of the other paralog. In order to confirm this observation, we also compared the *promNOOT2*::*GUS* fusion activity in *Mtnoot1* and wild type backgrounds (Magne et al., 2018a). In agreement with the *NBCL* gene expression analysis described above, the activity of this construct was overall similar in the two genotypes (**Supplementary Fig. S2**).

In *P. sativum*, *PsCOCH1* and *PsCOCH2* transcripts were detected in internodes, nodes, leaves, flowers and seeds (**Supplementary Fig. S1**). Both paralogs were generally co-expressed in the different organs tested, with *PsCOCH1* generally expressed at higher levels than *PsCOCH2*. Maximum expression of both genes was found in nodes, internodes and flowers. *PsCOCH1* and *PsCOCH2* were also more expressed in developing organs such as young leaves and young flowers suggesting a preponderant role for *PsCOCH* genes during early organ development. The expression data obtained for *P. sativum* are consistent with expression data retrieved from the *P. sativum* Gene Expression Atlas (PsGEA, http://bios.dijon.inra.fr/FATAL/cgi/pscam.cgi; Alves-Carvalho et al., 2015; **Supplementary Fig. S1D**).

Altogether, these results show that *NBCL* genes are often co-expressed in aerial organs with similar expression patterns in the two legume species, suggesting a possible functional redundancy and conserved functions of NBCL paralogs during different biological processes.

NBCL1 and *NBCL2* genes redundantly contribute to the development of stipules in *M. truncatula* and *P. sativum*

In wild type *M. truncatula,* a pair of stipules develops at the base of the leaf petiole. *M. truncatula* stipules have one to two digitations below the third stem node starting from the base of the plant. After the third node of older plants, the degree of serrations of these stipules increases and leads to more complex organs (**Fig. 2A**; **Supplementary Fig. S3A**). As previously described in the literature, stipules of the *Mtnoot1* mutants were simplified relative to wild type (**Fig. 2B; Supplementary Fig. S3B**; Couzigou *et al*., 2012). Here we show that in *Mtnoot2* mutants, stipules were not modified, while in the *Mtnoot1noot2* double mutant, the stipules were even more simplified than in *Mtnoot1* (**Fig. 2C, D; Supplementary Fig. S3C, D**).

By contrast to the simplified and stable stipule phenotype of *Mtnoot1* mutants, the *Mtnoot1noot2* stipules were all modified (**Fig. 2L**) and showed a range of shape variations (**Fig. 2D-K; Supplementary Fig. S3D-M**). Most *Mtnoot1noot2* stipules presented a needle-like structure that was often asymmetric in terms of position along the stem and shape, a phenomenon also observed in *Mtnoot1* (**Fig. 2D-F; Supplementary Fig. S3D-M**; Couzigou et al., 2012). In some cases, complex structures consisting of misplaced needle-like structures or abnormal leaflets or combinations of these structures, can be observed (**Fig. 2D-G; Supplementary Fig. S3D-M**). In *Mtnoot1noot2*, 18% of the stipules form leaf-like structures that often tend to be trifoliolated as a wild type leaf (**Fig. 2H-L; Supplementary Fig. S3J-M**). Some of these aberrant leaflets also displayed needle-like structures with modified serration on the leaf margin (**Supplementary Fig. S3G-I**). The size of these leaf-like structures was reduced compared to a true R-108 leaves (**Supplementary Fig. S3J-M)**. The *Mtnoot1noot2* stipule lamina of needle-like structures were two-fold longer in comparison to R-108, *Mtnoot1* or *Mtnoot2* single mutants (**Fig. 2A-D; Supplementary Fig. S3N-R**).

In wild type *P. sativum* (Caméor), stipules have a peltate morphology (**Fig. 2M**). In agreement with the literature, the development of *Pscoch1* stipules was strongly affected. The *Pscoch1* stipules show a range of mutant phenotypes, such as an absence of stipules, the presence of thread-like stipules, leaflet-like stipules (also called spoon-like) or compound leaf-like stipules (**Fig. 2N**; Gourlay et al., 2000; Yaxley et al., 2001; Kumar et al., 2009; Couzigou et al., 2012; Sharma and Kumar, 2013). In contrast, *Pscoch2* had wild-type stipules (**Fig. 2O**). In *Pscoch1coch2*, stipule modifications were similar to those observed in *Pscoch1* (**Fig. 2P**). To evaluate the implication of *PsCOCH2* in stipule development, the stipule morphology was checked node by node (from node 1 to 13, from bottom to top) in Caméor, *Pscoch1*, *Pscoch2* and *Pscoch1coch2* (**Fig. 2Q**). This analysis revealed that Caméor and *Pscoch2* only develop wild-type peltate stipules. *Pscoch1* generally lacked stipules from nodes 1 to 5, had thread-like stipules from nodes 6 to 7 and leaflet-like stipules from nodes 8 to 13. *Pscoch1coch2* displayed an increased stipule phenotype, mostly lacking stipules from nodes 1 to 9, having thread-like stipules at node 10 and leaflet-like stipules from nodes 11 to 13. These results show that the severity of stipule modification is increased in *Pscoch1coch2* compared to *Pscoch1* and reveal a role for *Pscoch2* in stipule development.

Taken-together, these results highlight redundant functions between NBCL1 and NBCL2 for stipule development in *P. sativum* and *M. truncatula*.

NBCL genes are involved in *P. sativum* leaf development but not in *M. truncatula*

As described above, *NBCL1* genes confer stipule identity but an eventual role in leaf development has not been reported. In wild type *M. truncatula*, *Mtnoot1*, *Mtnoot2* and *Mtnoot1noot2* mutant backgrounds, leaves are trifoliolate and indistinguishable from wild type suggesting that these genes do not participate in *M. truncatula* leaf development (**Fig. 3A-D;** Mo et al., 2022).

In wild type *P. sativum*, leaves from the first nodes have two proximal leaflets and a distal tendril (**Fig. 3E**). In *Pscoch1*, we occasionally observed some leaves with patterning defects, often limited to an additional proximal leaflet or a small leaflet associated with the distal tendril (**Fig. 3F, M**). In *Pscoch2*, leaves were identical to the wild type (**Fig. 3G**). In *Pscoch1coch2*, the majority of leaves were wild-type, but about 16% of the leaves had an increased leaf complexity (**Fig. 3M**). Aberrant leaves of *Pscoch1coch2* possessed more than two proximal leaflets and occasionally formed even more complex leaves with up to seven leaflets (**Fig. 3H; Supplementary Fig. S4**). On higher nodes, *Pscoch2* showed wild-type phenotype with at least two pairs of proximal leaflets and a terminal tendril (**Fig. 3I, K**). *Pscoch1* leaves showed additional leaflets and the *Pscoch1coch2* mutant occasionally produced complex leaves with more than five leaflets on later nodes (**Fig. 3J, L**).

The phenotypic analysis of *M. truncatula* and *P. sativum* leaf development shows that, in contrast to *MtNOOT1* and *MtNOOT2*, *PsCOCH2* gene seems to share a redundant function with *PsCOCH1* and likely contributes to the regulation of leaf development.

Legume *NBCL* genes are involved in the regulation of inflorescence architecture

In wild type *M. truncatula* and *Mtnoot1*, one-to-two flowers develop on a single inflorescence (**Fig. 4A, B; Supplementary Fig. S5A, B**). In contrast, *Mtnoot2* inflorescences bear more flowers per inflorescence compared to the wild type and *Mtnoot1*, and showed two-to-five flowers (**Fig. 4C; Supplementary Fig. S5A, B**). In *Mtnoot1noot2*, the number of flowers per inflorescence was increased compared to *Mtnoot2* and can reach up to ten or more flowers per inflorescence (**Fig. 4D; Supplementary Fig. S5A, B, F**). Some of these *Mtnoot1noot2* flowers occasionally showed an ectopic leaflet and a short or missing pedicel (**Supplementary Fig. S5C-F**). In addition, in contrast to the wild type or the single *Mtnoot1* and *Mtnoot2* mutants, multiple inflorescences were also observed at a single node of *Mtnoot1noot2* plants (**Fig. 4A-D**). We also found that *Mtnoot1noot2* floral peduncles were significantly longer than those of the wild type *M. truncatula* or *nbcl* single mutants (**Fig. 4I-J**). These results suggest that *MtNOOT1* and *MtNOOT2* redundantly contribute to the development of *M. truncatula* inflorescences.

P. sativum var. Caméor plants usually produce one-to-two flowers per inflorescence (**Fig. 4E**). *Pscoch1* mutants mostly had wild-type flowers however some inflorescences occasionally produced more than 3 flowers (**Fig. 4F**). *Pscoch2* strictly produced wild-type flowers (**Fig. 4G**). By contrast, *Pscoch1coch2* produced more flowers compared to *Pscoch1* with at least three flowers per inflorescence (**Fig. 4H**). In addition, the length of the *Pscoch1coch2* flower peduncles was significantly increased compared to wild type, *Pscoch1* and *Pscoch2* single mutants (**Fig. 4K-L**).

The increased flower number in *M. truncatula* and *P. sativum nbcl* double mutants indicates that the *NBCL* genes synergistically contribute to the development of the inflorescence and to the control of the number of flowers per inflorescence.

Legume *NBCL1* and *NBCL2* genes redundantly contribute to floral patterning

M. truncatula and *P. sativum* bear typical Papilionaceous flowers with five fused sepals and a corolla, made of one dorsal (adaxial) standard, two wings and two fused ventral (abaxial) petals, known as the keel, that covers the male and female reproductive parts of the flower. A central carpel is surrounded by 10 (9 fused and one free) anthers (**Fig. 5A, E, I, M; Fig. 6A, E, I, M**; Benlloch et al., 2003; Wang et al., 2008). In *M. truncatula*, flowers are subtended by a bract in ventral position and a dorsal residual stub, known as the spike, is produced by the residual activity of the secondary inflorescence meristem (Benlloch et al., 2003, 2015).

In *M. truncatula*, as previously described in the literature, *Mtnoot1* mostly developed wild-type flowers and occasionally formed flowers with additional sepals, petals and/or stamens (**Fig. 5B, F, J, N**; Couzigou et al., 2012). Here, we show that *Mtnoot2* mutant produced wild-type flowers (**Fig. 5C, G, K, O; Supplementary Fig. S6A, C, E, G**). In contrast, in *Mtnoot1noot2*, the development of flower was drastically altered with supernumerary sepals, petals, anthers and in some cases formation of a small pod-like structure (**Fig. 5D, H, L, P; Supplementary Fig. S9F, G**). In contrast to wild type, *Mtnoot1* and *Mtnoot2*, the *Mtnoot1noot2* juvenile flowers were prematurely opened (**Supplementary Fig. S6A-D**). This defect could explain the premature anther senescence observed in *Mtnoot1noot2* (**Supplementary Fig. S6H**). We also show that the length of the spike was significantly reduced in both *Mtnoot2* and *Mtnoot1noot2* producing an increased number of flowers per inflorescence as compared to wild type and *Mtnoot1* (**Supplementary Fig. S7A, B**). We also observed that the length of the bract was significantly increased in *Mtnoot1noot2* as compared to wild type and single mutants (**Supplementary Fig. S7A, C**). In addition, we noticed additional mutant phenotypes for *Mtnoot1noot2* flowers consisting of floral organ fusions between different floral whorls such

as between sepal and petal, petal and stamen, as well as between stamen and carpel whorls (**Supplementary Fig. S7D**). In conclusion, our observations suggest that NBCL1 and NBCL2 redundantly act to define floral whorls boundaries, and to control the number and the identity of floral organs formed.

In agreement with previous studies (Yaxley et al., 2001; Couzigou et al., 2012), *Pscoch1* flowers were often modified and contained additional sepals, petals, anthers and occasionally two central carpels were observed in *M. truncatula Mtnoot1noot2* flowers which can occasionally develop up to three carpels in a flower (**Fig. 6B, F, J, N; Supplementary Fig. S8A-L**). *Pscoch2* produced wild-type flowers (**Fig. 6C, G, K, O**). In *Pscoch1coch2*, the development of flowers was also impacted. The *Pscoch1coch2* floral phenotypes were similar to those of the single *Pscoch1* mutants however they were exacerbated with flowers showing supernumerary sepals, anthers and stigma (**Fig. 6D, H, L, P**).

In summary, our results show that in both *M. truncatula* and *P. sativum, nbcl1nbcl2* double mutants present stronger floral patterning defects relative to single *nbcl1* mutants. This suggests that *nbcl2* mutations increased the phenotype of the *nbcl1* mutants and that NBCL1 and NBCL2 are redundantly involved in *M. truncatula* and *P. sativum* flower development, especially for floral organs number and identity.

NBCLs regulate inflorescence and flower identity genes

The results presented above show that legume NBCLs are involved in the regulation of inflorescence and flower development. Legume floral organ identity, like in many flowering plants, can be explained by the ABC flower development model (Irish V., 2017). In *M. truncatula*, a homolog of *A. thaliana* class A *AtAPETALA1 (AtAP1*) genes, *MtAP1*, which is also known as *MtPIM (PROLIFERATING INFLORESCENCE MERISTEM),* specifies the floral meristem identity and represses flower-to-inflorescence transformations (Benlloch et al., 2006). In 2019, Zhao et al., also reported that loss-of-function of *MtAGAMOUS-LIKE FLOWER* (*MtAGLF*) gene resulted in modified flowers with stamens and carpel transformed into extra whorls of petals and sepals. In addition, the class C *MtAGAMOUSa* gene (*MtAGa*) has been shown as required for the control of stamen and carpel identity as well as for pod and seed development (Zhu et al., 2018). In *P. sativum*, the identity of primary inflorescence meristems is regulated by *PsDETERMINATE* (*PsDET*), an homolog of the *A. thaliana TFL1* genes (Foucher et al., 2003; Berbel et al., 2012) and the identity of floral meristems is controlled by *PsPROLIFERATING INFLORESCENCE MERISTEM* (*PsPIM*), the ortholog of the *A. thaliana AtAP1* gene (Berbel et al., 2001; Taylor et al., 2002; Berbel et al., 2012). Based on this

knowledge, we further analyzed the expression of these floral identity genes in the *nbcl* mutant flowers of *M. truncatula* and *P. sativum.*

The expression level of the *M. truncatula* floral identity genes *MtAP1*, *MtAGLF* and *MtAGa* was studied by RT-qPCR in *M. truncatula* flower primordia. In *Mtnoot1* and *Mtnoot2*, the expression of the three genes was not significantly different from wild type (**Fig. 5Q-S**). In *Mtnoot1noot2* flower primordia, the expression level of *MtAP1*, *MtAGLF* and *MtAGa* was significantly increased compared to wild type, *Mtnoot1* and *Mtnoot2* single mutants (**Fig. 5Q-S**).

These results highlight that in *M. truncatula*, *MtNOOT1* and *MtNOOT2* synergically regulate the expression of floral identity genes controlling flower determinacy.

Then, we studied the gene expression of the *PsDET* and *PsPIM* in the flower primordia and developing flower of wild type and *Pscoch1* mutants from three different *P. sativum* accessions (Caméor, JI2822 and SGE; **Fig. 6Q-T**; **Supplementary Fig. S8M-N**). We found that *PsPIM* was up-regulated in flower primordia and developed flowers from all *Pscoch1* lines (**Fig. 6Q and S; Supplementary Fig. S8M-N**). Similarly, *PsDET* was up-regulated in the flower primordia of all three *Pscoch1* lines as compared to the wild type. In contrast, *PsDET* was down-regulated in developed flowers when compared to the corresponding wild type backgrounds (**Supplementary Fig. S8M-N**). In *Pscoch2* flower primordia, only *PsDET* was found to be up-regulated while in developed flowers, *PsDET* and *PsPIM* were both up-regulated (**Fig. 6R**; **Supplementary Fig. S8M**). In *Pscoch1coch2* flower primordia, the increased *PsDET* expression level was comparable to that observed in *Pscoch1* (8-fold-changes; **Fig. 6R**) while the expression level of *PsDET* was significantly reduced in the developed flowers of *Pscoch1coch2* (**Supplementary Fig. S8M**). In contrast, in both the flower primordia and developed flowers of *Pscoch1coch2*, the gene expression level of *PsPIM* was significantly increased (**Fig. 6Q; Supplementary Fig. S8M**).

These results suggest that *Pscoch1* and *Pscoch1coch2* flowers are indeterminate and that *PsCOCH1* and *PsCOCH2* genes act as important upstream regulators of floral identity genes controlling flower determinacy and patterning.

Legume *NBCLs* control pod development and seed size

In agreement with the number of flowers per inflorescence, wild-type *M. truncatula* usually produced one, two and rarely three pods per inflorescence (**Fig. 7A**). The *Mtnoot1* mutant formed a single but larger pod per inflorescence compared to the wild type (**Fig. 7B**;

Supplementary Fig. S9A, B, E). As *Mtnoot2* usually produced more flowers per inflorescence, it generally produced three pods per inflorescence which were smaller than wild type (**Fig. 7A-C; Supplementary Fig. S9A-C, E**). *Mtnoot2* pod spikes were shorter than in R-108 and *Mtnoot1* (**Supplementary Fig. S9A-E)**. In contrast, *Mtnoot1noot2* mostly developed aborted pod-like structures and only a few pods that were reduced in size and with short pod spikes (**Fig. 7D; Supplementary Fig. S9A-E).** In *Mtnoot1*, seed width and length were increased compared to wild type and as a consequence, the weight of 100 *Mtnoot1* seeds was increased by 25% (**Fig. 7E, F**). By contrast, *Mtnoot2* seeds were smaller compared to wild type and consequently 14% lighter (**Fig. 7E, F**). *Mtnoot1noot2* pods only contained a few seeds that were bigger relative to wild type and the weight of 100 *Mtnoot1noot2* seeds was increased by 17% (**Fig. 7E, F**).

In *P. sativum*, *Pscoch1* tends to produce more pods than wild type that were mainly produced from lateral shoots (**Fig. 7J**). In agreement with the literature, *Pscoch1* pods were shorter and set few seeds that were bigger than wild type (1.4-fold; **Fig. 7G, H, J, K**; Yaxley et al., 2001). This reduced seed production was consistently observed in *Pscoch1*^{JI} and *Pscoch1*^{SGEapm} backgrounds producing mostly empty pods (**Supplementary Fig. S9K**). In *Pscoch2*, pods resembled wild-type pods with wild-type seed production, however the size of the seeds was reduced by 18% (**Fig. 7G, H, K**). *Pscoch1coch2* set a wild-type number of pods and seeds per plant but generally two-to-four pods formed on a single flower peduncle (**Fig. 7I, J; Supplementary Fig. S9H-J**). As observed for *Pscoch1*, seeds were bigger than in wild type (1.2-fold; **Fig. 7H, K**). The total seed weight per plant was significantly reduced in *Pscoch1* and *Pscoch2*, but tended to increase in *Pscoch1coch2* (**Fig. 7K**).

Although some variations were observed between *M. truncatula* and *P. sativum*, *NBCL1* and *NBCL2* show antagonistic functions in seed development with *NBCL1* and *NBCL2* negatively and positively contributing to seed size, respectively.

PsCOCH2 is required for *P. sativum* nodule development and functioning

In *M. truncatula*, *Mtnoot2* single mutant has no symbiotic phenotype. However, *Mtnoot2* plays an important role in nodule development since the *Mtnoot1noot2* mutant presents a more severe nodule-to-root phenotype compared to the single *Mtnoot1* mutant. *Mtnoot1noot2* is characterized by a complete loss of nodule identity and has lost the ability to fix nitrogen (Couzigou *et al.*, 2012; Magne *et al.*, 2018a).

In *P. sativum*, the function of *PsCOCH1* is conserved for the control of the symbiotic nodule identity (Ferguson and Reid, 2005; Couzigou *et al.*, 2012). RNAseq-based gene

expression data from the PsGEA revealed that both *PsCOCH1* and *PsCOCH2* genes are expressed in nodules, suggesting that *PsCOCH2* might also play a role in *P. sativum* nodule development and/or identity (**Fig. 8E;** Alves-Carvalho et al., 2015).

To confirm whether *PsCOCH2* is indeed expressed in nodules and to determine the role of *PsCOCH2* in nodule development, we analyzed the gene expression of *PsCOCH1* and *PsCOCH2* in root and nodules by RT-qPCR and performed nodulation assays using wild type, *Pscoch1*, *Pscoch2* and *Pscoch1coch2*.

In agreement with the RNA-seq data from PsGEA, we found that *PsCOCH1* and *PsCOCH2* were indeed strongly expressed and induced in nodules as compared to roots (**Fig. 8F**). As previously reported in the literature, nodulation assays reveal that 90% of the *Pscoch1* nodules were converted into root but still functional (pink coloration due to the presence of leghaemoglobin; **Fig. 8B, G;** Ferguson and Reid, 2005). In contrast, as previously shown for the *M. truncatula Mtnoot2* mutant, the *Pscoch2* nodules were similar to wild-type nodules and lacked any obvious mutant phenotype (**Fig. 8A, C, G**; Magne *et al*., 2018a). In *Pscoch1coch2,* a high frequency (90%) of nodules showing nodule-to-root conversions was observed, however, in comparison with the single *Pscoch1* nodules, the *Pscoch1coch2* nodules were poorly developed, three times smaller than wild-type nodules and were faintly pink to white suggesting that they were poorly to not functional for nitrogen fixation. Also, large pink mature nodules, converted or not, were not observed in *Pscoch1coch2* (**Fig. 8D, G, H**). In agreement with what is usually observed for nitrogen-fixing-deficient mutant legumes (Bourcy *et al*., 2013), *Pscoch1coch2* produced more nodule primordia and nodules than wild type, *Pscoch1* and *Pscoch2*, supporting that the *Pscoch1coch2* nodules were not efficiently fixing nitrogen (**Fig. 8H**). To verify this hypothesis, we thus assessed the nitrogen-fixing efficiency of *Pscoch* mutants using the Acetylene Reduction Assay (ARA). This analysis revealed that all the *Pscoch* mutants are efficiently fixing nitrogen (fix^+), however the *Pscoch1coch2* nitrogen fixation activity per nodule was significantly reduced relative to wild type in agreement with the observed nodule phenotypes (**Fig. 8I**).

These results show that, in *P. sativum*, *PsCOCH2,* together with *PsCOCH1*, are both required for symbiotic nodule development, identity maintenance and functioning. While nodule-to-root conversions are less frequent in *Mtnoot1* than in *Pscoch1*, our analysis reveals that, overall, both *NBCL1* and *NBCL2* gene functions are required for the proper development and functioning of the *M. truncatula* and *P. sativum* indeterminate nodules.

DISCUSSION

PsCOCH2 is orthologous to MtNOOT2

In this work, we characterized a new member of the Papilionoids-specific *NBCL2* clade, *P. sativum PsCOCH2* which is orthologous to *M. truncatula MtNOOT2* (Magne et al., 2018a). Using the TILLING-NGS technology we identified a KO mutant allele for the *PsCOCH2* gene locus that allowed comparing the function of these two *NBCL2* genes in two legume species. Furthermore, we used *Pscoch1coch2* and *Mtnoot1noot2* double mutants to evaluate the potential redundancy of *PsCOCH2* and *MtNOOT2* with *PsCOCH1* and *MtNOOT1,* respectively. Gene expression analysis revealed a strong transcriptional overlap between *MtNOOT1* and *MtNOOT2* in *M. truncatula* and between *PsCOCH1* and *PsCOCH2* in *P. sativum*. The two orthologous genes were co-expressed in many aerial organs, especially in leaves, stems and flowers in the two legume species, suggesting redundant functions in the regulation of aerial organ development.

NBCL2 participate in stipule and leave development and determinacy

In *A. thaliana*, the *AtBOP1* and *AtBOP2* genes are key regulators of the leaf morphogenesis and patterning (Ha et al., 2003; 2007) with *Atbop1bop2* mutant leaves showing extensive lobe formation and ectopic blade tissues along the petioles of cotyledons and leaves (Ha et al., 2003; Hepworth et al., 2005; Norberg et al., 2005; Ha et al., 2007). *A. thaliana* rosette leaves bear microscopic stipules, which are absent in the *Atbop1bop2* mutant (McKim et al. 2008). Conversely, *Atbop1bop2* cauline leaves are serrated at their base with structures strongly resembling stipules whereas wild type cauline leaves are smooth distally (Hepworth et al., 2005). In *S. lycopersicum*, three *BOP* genes participate in the diversity of leaf complexity through the repression of leaflet formation (Izhaki et al., 2018). Furthermore, in monocots, such as *H. vulgare*, *O. sativa* and *B. distachyon*, *NBCLs* are also required for the leaf ligule and auricles development (Tavakol et al., 2015; Jost et al., 2016; Toriba et al., 2019; Magne et al., 2020; Liu et al., 2021). The *Pscoch1* mutant was already described for stipule, flower and nodule developmental alterations and showed a strong penetrance (Yaxley et al., 2001; Ferguson and Reid, 2005; Couzigou et al., 2012). In contrast, *Mtnoot1* defects in *M. truncatula* aerial organs were mild, with reduced stipules and occasionally an increased petal number. The penetrance of the *Mtnoot1* mutation was also reduced for the symbiotic organ phenotypes in *M. truncatula* relative to *P. sativum* (Magne et al., 2018a). This indicates that *PsCOCH1* plays a more important role in *P. sativum* than *MtNOOT1* in *M. truncatula* for development highlighting the interest in studying orthologs in different plant species.

Interestingly, both *P. sativum* and *M. truncatula, nbcl2* single mutants lack particular aerial patterning defects, suggesting that the *NBCL1* genes may be sufficient for the development of the different aerial organs and that *NBCL2* genes can be dispensable. The *Pscoch1coch2* stipule and flower mutant phenotypes are similar to those of the single *Pscoch1* mutant. However, occasionally, *Pscoch1coch2* shows additional leaf developmental alterations characterized by an increased leaf complexity suggesting that *PsCOCH1* and *PsCOCH2* genes play a redundant function for leaf development and determinacy. In *M. truncatula,* the phenotyping of the single and double *nbcl* mutants shows that the *NBCL* genes are not participating in leaf development. The difference observed for the mutant leaf phenotypes between the two species suggests that *P. sativum* leaf development is partially undetermined, while *M. truncatula,* leaf development is determined.

Stipule modifications in *Pscoch1coch2* are similar to those of the *Pscoch1* single mutant; however, a detailed node by node analysis indicates that stipule development and identity are significantly more impacted in *Pscoch1coch2* relative to the *Pscoch1*. Indeed, while *Pscoch1* stipules are generally absent in the first five nodes, in *Pscoch1coch2* the absence of stipules is prolonged until the ninth node. These results show that the *PsCOCH2* gene is involved in stipule development and identity and that *PsCOCH2* is functionally redundant with *PsCOCH1* for stipule determinacy. In *Mtnoot1,* approximately 25% of the leaves from the two first nodes lack stipules, but overall, *Mtnoot1* stipules only display a reduced number of digitation and a reduced size at lower and higher node levels (Couzigou et al., 2012). In *Mtnoot1noot2,* stipule modifications are clearly enhanced and display a range of phenotypic variations, including compound leaf-like structures as seen in *Pscoch1* and *Pscoch1coch2* backgrounds. In young *Mtnoot1noot2* plants, stipules are highly reduced or even absent. On older plants, the length of the stipules is significantly increased and stipule-to-compound-leaf conversions are observed. Together, these results clearly indicate that members of the legume NBCL2 sub-clades play an important role for leaf and stipule development although with varying degrees in different species. Interestingly enough, *stip* (for modified stipules), a *nbcl1* mutant in *Lupinus angustifolius*, which is a basal Papilionoid, is also deficient for stipule development and abscission zone development (Clements et al., 2001; Couzigou et al., 2016), with absent stipules in the younger nodes (Couzigou et al. personal communication). In *L. japonicus* which bears nectaries at the leaf basis instead of stipules, the *nbcl1* mutant lacks leaf nectaries (Magne et al., 2018b). In conclusion, the Papilionoids NBCL and the *A. thaliana* AtBOP proteins, promote stipules development in younger nodes and rosette leaves, respectively, while they repress stipules development in older nodes and cauline leaves, respectively. Altogether, these

observations suggest an ancestral function for NBCL in regulating the development of stipules (or homologous structures such as nectaries in *L. japonicus*). Furthermore, the stipule phenotypes of *Mtnoot1noot2* are reminiscent of those observed in the *Mtphantastica* mutant (*Mtphan*; Zhou et al., 2014). This raises the possibility that in *M. truncatula*, MtPHAN and MtNOOT may interact together to regulate stipules development. Taken-together, this shows that the function of NBCL for the regulation of the leaf development and patterning is conserved in dicot and monocot.

NBCLs redundantly control legume inflorescence architecture

The inflorescence architecture is a main component of the huge diversity of forms found in flowering plants (Benlloch et al., 2015). Wild type *M. truncatula* and *Mtnoot1* generally produce one-to-three flowers per inflorescence. In contrast to the wild type and *Mtnoot1*, the number of flowers increases in *Mtnoot2* and can reach up to four flowers per inflorescence. In *Mtnoot1noot2*, the number of flowers per inflorescence is further increased with inflorescences carrying up to 10 flowers and a range of variations is observed. Also, in *Mtnoot1noot2*, the length of the flower inflorescence is increased. In line with these observations, we observed that the length of spikes and bracts was significantly reduced and increased, respectively. In *M. truncatula*, the inflorescence meristem 2 activity defines the number of flowers: it generally sets 1 or 2 floral meristems and then terminates into a spike (Benlloch et al., 2003; 2015). Here we show that *Mtnoot2* has smaller spike and that *Mtnoot1noot2* has no spike, a phenotype reminiscent of *Mtsuperman* also producing more flowers and having no spike (Rodas et al., 2021). As described for *Mtsuperman*, the *Mtnoot1noot2* phenotype suggests that the inflorescence meristem 2 activity duration is abnormally extended and this might explain the increased number of flowers compared to the wild type. In addition, the alteration of the *Mtnoot1noot2* floral determinacy and the floral organ fusions reflect the mis-establishment of the floral meristem which is also associated with the enlargement of the floral bract (Magne et al., 2018b). *Pscoch1* displays more flowers compared to wild type. In *Pscoch2*, the number of flowers per inflorescence and the length of the flower inflorescence are unchanged compared to wild type, whereas in *Pscoch1coch2* the number of flowers per inflorescence and the length of flower inflorescence are significantly increased. These results suggest that in legumes there is an additive effect of the *NBCL1* and *NBCL2* genes in the regulation of inflorescence architecture and determinacy.

As observed here for legumes, the three *S. lycopersicum SlBOPs* genes were also reported as acting together in the control of inflorescence architecture and flower production (Xu et al.,

2016). In agreement with their role in dicots, in grasses, the *H. vulgare NBCL* gene *HvLaxatum-a* (*HvLax-a*) also controls internode length and homeotic changes of the inflorescence, while its paralog *HvUniculme4* is apparently not involved in the control of the spike architecture (Tavakol et al., 2015; Jost et al., 2016). In *B. distachyon*, *BdCUL4* and *BdLAXA*, the orthologs of *HvCUL4* and *HvLAX-A*, are important for inflorescence development and for the control of spikelet determinacy (Magne et al., 2020). The differences between *A. thaliana* and other plants, including *M. truncatula*, *P. sativum*, *H. vulgare* and *B. distachyon* may result from an increased sub-functionalization of *NBCL1* and *NBCL2* homologs in the different species.

Legumes NBCL2 are involved in the regulation of floral patterning

The loss-of-function of *Atbop, Ntbop*, *Pscoch1* and *Mtnoot1* increases the number of floral organs, disturbs dorso-ventral floral patterning and alters flower symmetry (Yaxley et al., 2001; Ha et al., 2003; Hepworth et al., 2005; Norberg et al., 2005; Ha et al., 2007; Xu et al., 2010; Couzigou et al., 2012).

Flower modifications are subtle in *Mtnoot1*, suggesting a reduced penetrance of the *Mtnoot1* mutation in *M. truncatula* (Couzigou et al., 2012). *Mtnoot2* forms wild-type flowers while *Mtnoot1noot2* displays important floral alterations consisting of supernumerary sepals, petals, stamens and stigma which are accompanied by floral organ fusions. The malformation of the *Mtnoot1noot2* flowers leads to an open floral structure, to exposed stamens and to the premature anther senescence. In this mutant, carpels developed into non-fertile carpel structures leading to a drastic decrease in fertility (nearly sterile), a low pod set and a reduced number of seeds per pod. This phenotype is never observed in *Mtnoot1* highlighting that *MtNOOT2* plays a role in floral organ development. Taken-together, these phenotypes indicate that in *M. truncatula*, *MtNOOT1* and *MtNOOT2* are redundantly involved in the control of floral organ identity as well as in stamen and carpel development.

Typical *Pscoch1* flowers are dorsalized with supernumerary organs in all whorls (Yaxley et al., 2001; Kumar et al., 2011; Couzigou et al., 2012; Sharma et al., 2012). *Pscoch2* does not present any floral anomaly. The detailed analysis of the strength of the floral defects in *Pscoch1coch2* compared to *Pscoch1* revealed floral patterning alterations specific to *Pscoch1coch2*. Wild type *P. sativum* has ten anthers fused into a tube and one central carpel (Yaxley et al., 2001). *Pscoch1coch2* forms flowers with supernumerary sepals, petals, anthers and carpels. Most of these flowers have two central carpels and occasionally three or four. The absence of floral defects in *Pscoch2* suggests that *PsCOCH1* can compensate the loss-of-

function of *PsCOCH2* and that *PsCOCH2* and *PsCOCH1* have redundant roles during the early stages of *P. sativum* floral primordia development.

In *A. thaliana*, *AtBOP1, AtBOP2, AtLEAFY* (*AtLFY*) and *AtAPETALA1* (*AtAP1*) activities converge in blocking the continued expression of inflorescence meristem identity genes to maintain floral meristem determinacy (Liu et al., 2009; Xu et al., 2010; Chahtane et al., 2018). *AtBOP1, AtBOP2* also indirectly repress the expression of *AtAP1* during organ boundary definition (Khan et al., 2015). The gene expression of the *AtAP1* ortholog *in P. sativum*, *PsPIM*, was slightly upregulated in *Pscoch1* and *Pscoch1coch2* mutant flower primordia, and significantly increased in developed flowers (Taylor et al., 2002). In line with this, *PsDET*, which maintains apical meristem indeterminacy during flowering is significantly upregulated in *Pscoch1* and *Pscoch1coch2* flower primordia, and decreased in developed flowers (Foucher et al., 2003). This shows that *PsCOCH1* promotes floral meristem determinacy through the repression of *PsDET*.

In *M. truncatula*, the expression of the flower identity genes *MtAP1* and *MtAGa* is negatively controlled by *MtNOOT1* and *MtNOOT2*, showing the role of *NBCL* genes in controlling legume flower development in agreement with the work of Khan et al. (2015) in *A. thaliana* showing an ATH1/KNAT6 mediated negative control of AP1 by BOP1 and BOP2. In addition, in *Mtnoot1Mtnoot2*, the over expression of these genes compared to that in the single mutants, correlates with the strength of the floral phenotype.

Our results are in agreement with the literature reporting on the role of NBCLs in the regulation of inflorescence and floral meristem fate acquisition and development, and highlight that, in legume, NBCLs repress inflorescence indeterminacy and positively contribute to flower organ identity and development (Khan et al., 2014; Hepworth and Pautot, 2015; Khan et al., 2015).

The NBCL clade supports a conserved function in **governing fruit architecture**

Plant seeds represent primary food resources for both human diet and animal feeding. During crop domestication, seed size represented a major agronomic trait for selection (Linkies et al., 2010; Li and Li, 2014; Li and Li, 2016). Legume seeds are a major source of dietary proteins and oils (Ge et al., 2016). Preliminary evidences suggest that AtBOP1 and AtBOP2 activities govern fruit architecture. In *A. thaliana* fruits, AtBOP1, AtBOP2, AtKNAT6 and AtKNAT2 function in the same regulatory pathway as evidenced by the rescue of the replum mis-formation in *Atpennywise* (*Atpny)* mutants by either *bop1 bop2* or *knat2 knat6* loss-of-functions (Ragni et al., 2008; Khan et al., 2012a). Given that AtBOP1/2 act via KNAT6-ATH1

in the stem and abscission zone, this regulatory module would likely pattern fruit architecture (Khan et al., 2012b).

In *M. truncatula*, *Mtnoot1* has an increased pod size and larger seeds. In contrast, *Mtnoot2* pod and seed size were reduced maybe because the number of pods per inflorescence was increased. In *Mtnoot1noot2*, pod number and size were also significantly reduced. *Mtnoot1noot2* only produces a few pods filled with larger seeds, revealing a role for MtNOOT in the control of seed size.

In agreement with previous studies, we show that the number of seeds is reduced in *Pscoch1* (Yaxley et al., 2001). In addition, we found that *Pscoch1* seed size is increased. However, as each pod produces only one or two seeds, this can result in larger seeds. In *Pscoch2*, the seed size and weight are reduced, consistently with the *Mtnoot2* phenotype. Also, as observed for *Pscoch1*, *Pscoch1coch2* seed size is increased while producing a number of seeds comparable to wild type. These results indicate a role for PsCOCH in the control of seed size.

Together, this indicates that legume *NBCLs* share conserved functions in fruit development with possible antagonistic actions between NBCL1 and NBCL2 in controlling seed size.

PsCOCH2 is required for *P. sativum* indeterminate nodule development, identity maintenance and functioning

The *Mtnoot2* single mutant was reported as having no particular symbiotic phenotype while sharing a redundant function with *MtNOOT1* for *M. truncatula* nodule development and identity maintenance, since *Mtnoot1noot2* shows a complete loss of nodule identity characterized by a complete reversion of the nodules into roots and a fix minus phenotype (Magne et al., 2018a).

As previously reported for *Mtnoot2* in *M. truncatula*, in this study, we show that *PsCOCH2* is not expressed in the root while highly induced in nodules and that *Pscoch2* has no symbiotic phenotype.

The *Pscoch1* mutants already displays a very strong nodule-to-root conversion phenotype which likely does not affect symbiotic performance (≈90% of converted nodules; this study; Fergusson and Reid, 2005; Couzigou et al., 2012; Couzigou and Ratet, 2015). *Pscoch1coch2* also showed a very strong nodule-to-root conversion phenotype (≈90% of converted nodules), but presented additional nodule developmental defects. *Pscoch1coch2* produces only small and early-converted nodules showing faint pink to white coloration that were supernumerary

compared to the wild type and the single mutants. Moreover, symbiotic performance assessment revealed a reduced nitrogenase activity in the nodules of *Pscoch1coch2*.

Our results show that the loss-of-function of both *PsCOCH1* and *PSCOCH2* impairs nodule development and identity and leads to a reduced nitrogen fixation per nodule probably associated to a reduced rhizobial colonization as a consequence of this altered development. The *Pscoch1coch2* supernumerary nodule phenotype is typical of the increased nodule number observed in fix- plant mutants (Bourcy et al., 2013) and suggests that the nodules formed on the double mutant are not perceived as fully functional nodules by the plant. These results confirm the role of the legume specific *NBCL2* genes in symbiotic organ development and identity.

NBCL2, a legume invention

As described for other species, this study shows that *NBCL1* and *NBCL2* genes likely have unequal redundant functions depending on a given vegetative or reproductive developmental process. For example, whereas *A. thaliana* AtBOP1 seems to have a more prominent role in leaf development than AtBOP2, AtBOP2 has a more prominent function during reproductive growth (Khan et al. 2014). Our study also suggests that the respective function of the two NBCL clades can vary between a given organ and between legume species, highlighting the interest in studying these genes in different legume species. MtNOOT2 and PsCOCH2 belong to the unexplored legume-specific NBCL2 sub-clade and now represent the first characterized members of this sub-clade. We have shown that *NBCL2* participate in the development and the determinacy of the stipules and leaves, and highlighted that *NBCL2* are involved in the regulation of the inflorescence architecture and floral patterning. Shen et al. (2020) have recently shown that inside the legume family different legume clades (Papilionoideae and Caesalpinioideae) have independently duplicated a common *NBCL* ancestor gene. In agreement with this, our work support the hypothesis that *NBCL2* has evolved in the Papilionoideae clade from the more ancient and more polyvalent *NBCL* ancestral sequence to fulfill other functions in legume development and/or to create additional regulatory steps to better control plant developmental processes, such as for example, the establishment of the root nodule organogenesis. Our work also highlights that the two legume *NBCL* paralogs can have either complementary or antagonistic roles during development. *AtBOP1* and *AtBOP2* belong to the *NBCL* clade and their role in tissue boundaries establishment and functioning is well known and described in *A. thaliana*. Thus, similar roles for the legume *NBCL* genes in the

regulation of organ boundaries, adjacent organ establishment, size and identity would be coherent.

The legume *nbcl* single and double mutants described here represent important genetic tools to further study the role of *NBCL* and to precise their functions in the molecular networks underlying nodule, stipule, leaf and flower development, patterning and identity in legumes, as the *Atbop* single and double mutants have been exploited in *A. thaliana* over the past decades.

Supplementary data The following supplementary data are available at *JXB* online.

Supplementary Fig. S1. *NBCLs* gene expression patterns in *M. truncatula* and *P. sativum*

Supplementary Fig. S2. *MtNOOT2* spatial expression in aerial parts of *M. truncatula* R-108 and *Mtnoot1* backgrounds.

Supplementary Fig. S3. Stipule phenotypes of the *M. truncatula* single and double *nbcl* mutants.

Supplementary Fig. S4. *Pscoch1coch2* leaf phenotypes

Supplementary Fig. S5. Inflorescence phenotypes in R-108, *Mtnoot1*, *Mtnoot2* and *Mtnoot1noot2*.

Supplementary Fig. S6. Histological analysis of juvenile flowers of R-108, *Mtnoot1*, *Mtnoot2* and *Mtnoot1noot2*.

Supplementary Fig. S7. Spike and bract length, and occurrence of floral organ fusions in the *M. truncatula nbcl* mutants.

Supplementary Fig. S8. Floral organization in *Pscoch1*^{SGEapm} and *Pscoch1*^{JI} and flower developmental marker genes expression.

Supplementary Fig. S9. *M. truncatula* and *P. sativum* mutant pods phenotypes.

Supplementary Table S1. Overview of the mutations identified for the *PsCOCHLEATA2* locus by TILLING-NGS

Supplementary Table S2. Mutations identified for the *PsCOCHLEATA2* gene by TILLING-NGS

Supplementary Table S3. Segregation analysis of the *PsCOCH2 Ps1178* locus

Supplementary Table S4. Segregation analysis of double mutants heterozygous for the independent and recessive *PsCOCH1* and the *PsCOCH2* locus

Supplementary table S5. Oligonucleotides used for TILLING-NGS screen and genotyping

Supplementary Table S6. Primers used for RTqPCR

Acknowledgments

Shengbin Liu was supported by a 4- year Chinese scholarship council PhD scholarship (CSC grant no 201608510056). JZ was supported by China Scholarship Council (CSC) (grant no. 2019069900236) carried out in the SEVAB doctoral program (UPS, Toulouse, France).

Author contributions

SL, KM, JMC and PR conceived the research plan. SL, KM, JZ and JMC designed the experiments. SL, KM, JZ, JMC and JL performed the research experiments and analyzed the data. CLS and RT produced the *P. sativum* TILLING population. AB and MD developed the TILLING-NGS strategy. SL, KM, JMC and PR wrote the article.

Conflict of interest

The authors have no conflicts of interest to declare.

Funding

This work was supported by the CNRS and by a grant (ANR-14-CE19-0003-01) from the French National Research Agency to PR. This work has benefited from the support of the LabEx Saclay Plant Sciences (ANR-10-LABX-0040-SPS, LabEx SPS and ANR-17-EUR-0007, EUR SPS-GSR) which is managed by the French National Research Agency under the program ‘Investissements d’avenir’ (ANR-11-IDEX-0003-02). JMC and JZ were supported by the French Laboratory of Excellence project "TULIP" (ANR-10-LABX-41; ANR-11-IDEX-0002-02).

Data availability

All data supporting the findings of this study are available within the paper and within its supplementary materials published online.

Fig. 1. Genetic material used in this study and *NBCL* gene structure.

A, genetic characteristics and name of the different *nbcl* mutant lines used in this study. **B**, schematic representation of the *NBCL* gene and protein structures. Rectangles and lines represent exons and intron, respectively. The positions of the mutations are indicated on the gene structure for the *M. truncatula Tnt1* insertions and on the protein structure for the *P. sativum* point mutations.

Fig. 2. *M. truncatula* and *P. sativum* single and double *nbcl* mutants stipule phenotypes

A-K, stipules of wild type *M. truncatula* R-108 (A), *Mtnoot1* (B), *Mtnoot2* (C) and *Mtnoot1noot2* (D-K) mutants. In R-108, the stipules developing at the base of the petiole have several serrations above node 3 (A). *Mtnoot1* stipules present a reduced serration (B), *Mtnoot2* stipules are not different from the wild type (C), the *Mtnoot1noot2* stipules present a range of alterations and mostly present a needle-like structure (D). **E-K**, the other *Mtnoot1noot2* stipule phenotypes include leaflet-like stipules or branched stipules. **L**, quantification of the needle-like and stipule-to-leaf conversions in *Mtnoot1noot2*. The frequency was calculated from 4 adult plants (n=800 pairs of stipules). Stars indicate wild-type stipules, asterisks indicate needle-like stipules and arrowheads indicate stipule-to-leaf conversions. **M-P**, stipules of wild type *P. sativum* Caméor (M), *Pscoch1* (N), *Pscoch2* (O) and *Pscoch1coch2* (P). Caméor and *Pscoch2* have wild-type peltate stipules while *Pscoch1* and *Pscoch1coch2* show a range of stipule phenotypes. Stipules can be either absent (Ab), thread-like (Th), leaf like (Lf) or compound leaf-like (Cl). Scale bars **A-K** and **M-P**: 1 cm. **Q**, schematic representation of the stipule morphology alterations in the *P. sativum nbcl* mutants. Stipule morphology is reported from node 1 to 13 (from the bottom to the top of the plant, left axis) in Caméor, *Pscoch1*, *Pscoch2* and *Pscoch1coch2*. Stipule morphologies were classed into four categories: wild-type peltate stipules (Wt, green), leaflet-like or compound leaf-like stipules (Lf, light pink), thread-like stipules (Th, red) and absence of stipule (Ab, dark red). Values represent mean percentage for each stipule category. For each genotype and for each node, the most represented stipule category is highlighted with the corresponding color. n, number of stipules analyzed per node position. Caméor, 7 plants; *Pscoch1*, 7 plants; *Pscoch2*, 5 plants; *Pscoch1coch2*, four lines from independent crossing, 28 plants.

Fig. 3. *M. truncatula* and *P. sativum* single and double *nbcl* mutants leaf phenotypes

A-D, *M. truncatula* R-108 (A), *Mtnoot1* (B), *Mtnoot2* (C) and *Mtnoot1noot2* (D) leaf phenotypes. The single and double *M. truncatula nbcl* mutants have wild-type leaves. **E-L,** basal node (E-H) and upper nodes (I-L) leaf phenotypes in *P. sativum* Caméor (E, I), *Pscoch1* (F, J), *Pscoch2* (G, K) and *Pscoch1coch2* (H, L). **E**, basal Caméor leaves have two leaflets and distal tendrils. **F**, basal *Pscoch1* leaves mainly show wild-type leaf leaves but occasionally display additional leaflets. **G**, basal *Pscoch2* leaves show wild-type leaf phenotype. **H**, basal *Pscoch1coch2* leaves mainly show wild-type leaves but occasionally display an increased leaf complexity with additional leaflets. **I**, upper Caméor compound leaves present at least two pairs of leaflets and a distal tendril. **J**, upper *Pscoch1* leaves mainly show wild-type leaves but occasionally display additional leaflets. **K**, upper *Pscoch2* leaves show a wild-type leaf phenotype. **L**, upper *Pscoch1coch2* leaves mainly show wild-type leaves but occasionally display additional leaflets. Pictures A-D showing *M. truncatula* leaf morphology have also been used in Supplementary Fig. S3 to illustrate the morphology of stipules. Scale bars **A-L**: 1 cm. **M**, quantification of the increased leaf complexity in Caméor, *Pscoch1*, *Pscoch2* and *Pscoch1coch2* backgrounds.

Fig. 4. *M. truncatula* and *P. sativum* single and double *nbcl* mutants inflorescence phenotypes.

A-D, I, *M. truncatula* R-108 (A), *Mtnoot1* (B), *Mtnoot2* (C) and *Mtnoot1noot2* (D) inflorescence phenotypes. The insert in (C) highlight an inflorescence with multiple young flowers. **E-H, K**, *P. sativum* Caméor (E), *Pscoch1* (F), *Pscoch2* (G) and *Pscoch1coch2* (H) inflorescences phenotypes. Scale bars **A-H**, **I** and **K**: 1 cm. **J, L** average length of the inflorescence in the *M. truncatula* and *P. sativum nbcl* mutant backgrounds.

Fig. 5. *M. truncatula nbcl* mutant flower phenotypes and floral identity marker genes expression.

A-D, *M. truncatula* R-108 (A), *Mtnoot1* (B), *Mtnoot2* (C), and *Mtnoot1noot2* (D) flowers. **E-P**, dissection of R-108 (E, I, M), *Mtnoot1* (F, J, N), *Mtnoot2* (G, K, O), and *Mtnoot1noot2* (H, L, P) floral organs. *M. truncatula* R-108 shows closed flower composed by five sepals, five petals, one carpel and ten stamens (A, E, I, M). *Mtnoot1* shows occasionally open flowers with a range of floral patterning defects including increased number of petals and petal identity defects (B, F, J, N). *Mtnoot2* flowers are not different from the wild type (C, G, K, O). *Mtnoot1noot2* shows mostly open flowers and strong floral patterning defects (D, H, L, P). *Mtnoot1noot2* shows flowers with supernumerary petals (H), the central carpel not well

enclosed by stamens (L) and the number of sepal teeth is increased (P) Scale bars **A-H**: 500 µm, **I-P**: 200 µm. St, standard; w, wing; k, keel; s, sepal; pe, pedicel; ste, stamen; sti, stigma. **Q-S**, RT-qPCR gene expression of the floral marker genes *MtAP1* (Q), *MtAGLF* (R) and *MtAGa* (S) in R-108, *Mtnoot1*, *Mtnoot2* and *Mtnoot1noot2* mutant flowers. Gene expressions were normalized against reference genes and normalized against R-108 control plants. *, p-value < 0.05; **, p-value < 0.01; Mann and Whitney test. Data represent means ± SE (n = 3).

Fig. 6. *P. sativum nbcl* mutant flower phenotypes and floral identity marker genes expression.

A-D, *P. sativum* Caméor (A), *Pscoch1* (B), *Pscoch2* (C) and *Pscoch1coch2* (D) flowers. **E-P**, dissection of Caméor (E, I, M), *Pscoch1* (F, J, N), *Pscoch2* (G, K, O) and *Pscoch1coch2* (H, L, P) floral organs. Caméor shows closed flower composed by five sepals, five petals, on carpel and ten stamens (A, E, I, M). *Pscoch1* shows mostly open flowers with a range of floral patterning defects consisting in an increased number of sepals, petals and stamen number, in floral organ fusions, as well as in floral organ identity defects and a loss of flower symmetry (B, F, J, N). *Pscoch2* flowers are not different from the wild type (C, G, K, O). *Pscoch1coch2* shows similar but stronger floral patterning defects than *Pscoch1*. Most *Pscoch1coch2* flowers are open with supernumerary sepals and petals and fused floral organs (D, H, L, P). St, standard; w, wing; k, keel; s, sepal; pe, pedicel; ste, stamen; sti, stigma. Dotted lines represent symmetry. Scale bars **A-H**, **M-P**: 500 µm; **I-L**: 200 µm. **Q-T**, RT-qPCR gene expression of the floral marker genes *PsPIM* and *PsDET* in flower primordia of Caméor, *Pscoch1*, *Pscoch2* and *Pscoch1coch2* (Q, R) and in flower primordia of JI2822, $Pscoch1^{JI}$ and SGE, $Pscoch1^{SGEapm}$ backgrounds (S, T). Gene expressions were normalized against reference genes and normalized against Caméor, JI2822 or SGE control plants. *, p-value < 0.05; **, p-value < 0.01; Mann and Whitney test. Data represent means ± SE (n = 3).

Fig. 7. *M. truncatula* and *P. sativum* single and double *nbcl* mutants pod and seed phenotypes.

A-D. global views of *M. truncatula* R-108 (A), *Mtnoot1* (B), *Mtnoot2* (C), and *Mtnoot1noot2* (D) pods. *Mtnoot1* pods are bigger than wild type pods. *Mtnoot2* pods are smaller than wild type pods and *Mtnoot2* produces more pods per inflorescence. *Mtnoot1noot2* pods are smaller than wild type pods. **E**, seed size of *Mtnoot1*, *Mtnoot2* and *Mtnoot1noot2* compared to R-108. **F**, seed weight for 100 seeds of R-108, *Mtnoot1*, *Mtnoot2*, and *Mtnoot1noot2*. **G**, global views of Caméor (left), *Pscoch1* (middle left), *Pscoch2* (middle right) and *Pscoch1coch2* (right) pods.

Pscoch1 shows abnormal pods while *Pscoch2* and *Pscoch1coch2* look-like wild type pods. **H**, seed size of Caméor (top), *Pscoch1* (upper middle), *Pscoch2* (lower middle) and *Pscoch1coch2* (bottom). **I**, *Pscoch1coch2* produces more (2 to 4) pods per inflorescence. **J-K**, number of pods, seeds (J) and seed weight (K) in Caméor, *Pscoch1*, *Pscoch2* and *Pscoch1coch2*. *, p-value < 0.05; **, p-value < 0.01; Mann and Whitney test. Scale bars **A-D, G-I**: 1 cm, **E**: 1mm.

Fig. 8. *P. sativum* single and double *nbcl* mutants nodule phenotypes and nitrogen fixation efficiency.

A-D, 35 days post-inoculation root nodules from Caméor (A), *Pscoch1* (B), *Pscoch2* (C) and *Pscoch1coch2* (D) inoculated with *R. leguminosarum* strain P221. **A**, Caméor forms indeterminate pink nodules. **B**, *Pscoch1* forms pink nodules that convert into root organs (white asterisks). **C**, *Pscoch2* forms indeterminate pink nodules comparable to Caméor. **D**, *Pscoch1coch2* nodules show tiny white-to-light pink nodules that convert into root organs (white asterisks). Big pink nodules shown in **A, B, C**, were not observed in *Pscoch1coch2*. **E**, **F**, RNAseq- (E) and RT-qPCR- (F) based gene expression of *PsCOCH1* and *PsCOCH2* in Caméor root and nodules. Data presented in panel (F) represent means ± SE of three biological replicates. **G,** nodule-to-root conversion penetrance in Caméor, *Pscoch1*, *Pscoch2* and *Pscoch1coch2*. Results represent mean percentages ± SE. Wild-type nodules and converted nodules are represented by the pink bars and the red bars, respectively. Caméor and *Pscoch2* only present wild-type nodules while *Pscoch1* and *Pscoch1coch2* present 90% of converted nodules (nodule primordia are not represented here). **H,** number and phenotype of the nodules per plant in Caméor, *Pscoch1*, *Pscoch2* and *Pscoch1coch2*. Caméor and *Pscoch2* only show wild-type nodules and nodule primordia. *Pscoch1* mostly forms nodules converted into root with a few wild-type nodules and nodule primordia. *Pscoch1coch2* shows an increased number of nodules with twice more converted nodules than *Pscoch1* and twice more nodule primordia than Caméor or *Pscoch2*. **I**, nitrogen fixation efficiency per nodule (nodule primordia were not taken into account for the normalization) in Caméor, *Pscoch1*, *Pscoch2* and *Pscoch1coch2*. Asterisks indicate significant difference compared to Caméor, **, p-value < 0.01; Mann and Whitney test. Results in (**G, H** and **I**) represent means ± SE of one biological experiment containing 4 plants for Caméor, *Pscoch1*, *Pscoch2* and 16 plants from four independent crossings for *Pscoch1coch2* representing 612 Caméor nodules, 422 *Pscoch1* nodules, 511 *Pscoch2* nodules and 5172 *Pscoch1coch2* nodules. Scale bars **A-D,** 500 µm.

Literature cited:

Assis R, Bachtrog D. (2013) Neofunctionalization of young duplicate genes in Drosophila. Proc Natl Acad Sci U S A. **110**(43):17409-14

Alves-Carvalho S, Aubert G, Carrère S, Cruaud C, Brochot AL, Jacquin F, Klein A, Martin C, Boucherot K, Kreplak J, et al (2015) Full-length de novo assembly of RNA-seq data in pea (*Pisum sativum* L.) provides a gene expression atlas and gives insights into root nodulation in this species. Plant J **84**: 1–19

Benlloch R, Berbel A, Ali L, Gohari G, Millán T, Madueño F (2015) Genetic control of inflorescence architecture in legumes. Front Plant Sci **6**: 1–14

Benlloch R, d'Erfurth I, Ferrandiz C, Cosson V, Beltran JP, Canas LA., Kondorosi A., Madueno F, Ratet P (2006) Isolation of mtpim proves Tnt1 a useful reverse genetics tool in *Medicago truncatula* and uncovers new aspects of AP1-Like functions in Legumes. Plant Physiol **142**: 972–983

Benlloch R, Navarro C, Beltrán JP, Cañas LA (2003) Floral development of the model legume *Medicago truncatula*: Ontogeny studies as a tool to better characterize homeotic mutations. Sex Plant Reprod **15**: 231–241

Berbel A, Ferrándiz C, Hecht V, Dalmais M, Lund OS, Sussmilch FC, Taylor S a., Bendahmane A, Ellis THN, Beltrán JP, et al (2012) VEGETATIVE1 is essential for development of the compound inflorescence in pea. Nat Commun **3**:797

Berbel A, Navarro C, Ferŕndiz C, Cañas LA, Madueño F, Beltrán JP (2001) Analysis of PEAM4, the pea AP1 functional homologue, supports a model for AP1-like genes controlling both floral meristem and floral organ identity in different plant species. Plant J **25**: 441–451

Blixt S (1967) Linkage studies in Pisum.VII. the manifestation of the genes *CRI* and *COCH* and the double recessive in *Pisum*. Agric Hortic Genet **25**: 131–144

Bourcy M., Brocard L., Pislariu C.I., Cosson V., Mergaert P., Tadege M., Mysore K.S., Udvardi M.K., Gourion B., Ratet P. (2013) *Medicago truncatula* DNF2 is a PI-PLC-XD-containing protein required for bacteroid persistence and prevention of nodule early senescence and defense-like reactions. New Phytol **197**(4), 1250-61**Canet JV, Dobón A, Fajmonová J, Tornero P**. (2012) The BLADE-ON-PETIOLE genes of Arabidopsis are essential for resistance induced by methyl jasmonate. BMC Plant Biol. **12**:199. doi: 10.1186/1471-2229-12-199.

Chahtane H, Zhang B, Norberg M, LeMasson M, Thévenon E, Bakó L, Benlloch R, Holmlund M, Parcy F, Nilsson O, et al (2018) LEAFY activity is post-transcriptionally

regulated by BLADE ON PETIOLE2 and CULLIN3 in Arabidopsis. New Phytol **220**: 579–592

Clements J, Atkins C. (2001) Characterization of a non-abscission mutant in *Lupinus angustifolius*. I. Genetic and structural aspects. American Journal of Botany **88**: 31–42

Couzigou J-M, Zhukov V, Mondy S, Abu el Heba G, Cosson V, Ellis THN, Ambrose M, Wen J, Tadege M, Tikhonovich I, et al (2012) NODULE ROOT and COCHLEATA maintain nodule development and are legume orthologs of Arabidopsis BLADE-ON-PETIOLE genes. Plant Cell **24**: 4498–4510

Couzigou JM, Magne K, Mondy S, Cosson V, Clements J, Ratet P (2016) The legume NOOT-BOP-COCH-LIKE genes are conserved regulators of abscission, a major agronomical trait in cultivated crops. New Phytol **209**: 228–240

Dalmais M, Schmidt J, Le Signor C, Moussy F, Burstin J, Savois V, Aubert G, Brunaud V, de Oliveira Y, Guichard C, Thompson R, Bendahmane A (2008) UTILLdb, a *Pisum sativum* in silico forward and reverse genetics tool. Genome Biol. **9(2)**: R43

Ding Y, Dommel M, Mou Z. (2016) Abscisic acid promotes proteasome-mediated degradation of the transcription coactivator NPR1 in *Arabidopsis thaliana*. Plant J. **86**(1): 20-34

Dong X. (2004) NPR1, all things considered. Curr Opin Plant Biol. **7**(5):547-52.

Dong Z, Li W, Unger-Wallace E, Yang J, Vollbrecht E, Chuck G (2017) Ideal crop plant architecture is mediated by tassels replace upper ears1, a BTB/POZ ankyrin repeat gene directly targeted by TEOSINTE BRANCHED1. Proc Natl Acad Sci USA **114**(41): E8656–E8664

Ferguson BJ, Reid JB (2005) Cochleata: Getting to the root of legume nodules. Plant Cell Physiol **46**: 1583–1589

Foucher F, Morin J, Courtiade J, Cadioux S, Ellis N, Banfield MJ, Rameau C, Génétique D, National I, Recherche D, et al (2003) DETERMINATE and LATE FLOWERING are two TERMINAL FLOWER1 / CENTRORADIALIS homologs that control two distinct phases of flowering initiation and development in Pea. Plant Cell **15**: 2742–2754

Ge L, Yu J, Wang H, Luth D, Bai G, Wang K, Chen R (2016) Increasing seed size and quality by manipulating BIG SEEDS1 in legume species. PNAS **113**: 12414–12419

Gourlay CW, Hofer JM, Ellis TH (2000) Pea compound leaf architecture is regulated by interactions among the genes UNIFOLIATA, cochleata, afila, and tendril-lessn. Plant Cell **12**: 1279–94

Ha CM, Jun JH, Nam HG, Fletcher JC (2007) BLADE-ON-PETIOLE1 and 2 control Arabidopsis lateral organ fate through regulation of LOB domain and adaxial-abaxial polarity genes. Plant Cell **19**: 1809–1825

Ha CM, Kim GT, Kim BC, Jun JH, Soh MS, Ueno Y, Machida Y, Tsukaya H, Nam HG (2003) The BLADE-ON-PETIOLE 1 gene controls leaf pattern formation through the modulation of meristematic activity in Arabidopsis. Development **130**: 161–172

Hepworth SR, Pautot VA (2015) Beyond the Divide: Boundaries for Patterning and Stem Cell Regulation in Plants. Front Plant Sci **6**: 1–19

Hepworth SR, Zhang Y, McKim S, Li X, Haughn GW (2005) BLADE-ON-PETIOLE-dependent signaling controls leaf and floral patterning in Arabidopsis. Plant Cell **17**: 1434–1448

Hoffmann B, Trinh TH, Leung J, Kondorosi A, Kondorosi E (1997) A new *Medicago truncatula* line with superior *in vitro* regeneration, transformation, and symbiotic properties isolated through cell culture selection. Mol Plant-Microbe Interact **10**: 307–315

Ichihashi Y, Aguilar-Martınez JA, Farhi M, Chitwood DH, Kumar R, Millon LV, Peng J, Maloof JN, Sinha NR (2014) Evolutionary developmental transcriptomics reveals a gene network module regulating interspecific diversity in plant leaf shape. Proc Natl Acad Sci USA **111**: E2616–E2621

Irish V. (2017) The ABC model of floral development. Curr Biol. **27**(17):R887-R890. doi: 10.1016/j.cub.2017.03.045.

Izhaki A, Alvarez JP, Cinnamon Y, Genin O, Liberman-Aloni R, Eyal Y (2018) The tomato BLADE ON PETIOLE and TERMINATING FLOWER regulate leaf axil patterning along the proximal-distal axes. Front Plant Sci **9**: 1–10

Jing R, Vershinin A, Grzebyta J, Shaw P, Smýkal P, Marshall D, Ambrose MJ, Ellis TH, Flavell AJ (2010) The genetic diversity and evolution of field pea (Pisum) studied by high throughput retrotransposon based insertion polymorphism (RBIP) marker analysis. BMC Evol Biol. **10**:44

Jost M, Taketa S, Mascher M, Himmelbach A, Yuo T, Shahinnia F, Rutten T, Druka A, Schmutzer T, Steuernagel B, et al (2016) A homolog of Blade-On-Petiole 1 and 2 (BOP1/2) controls internode length and homeotic changes of the barley inflorescence. Plant Physiol **171**(2): 1113-1127

Khan M, Xu H, Hepworth SR (2014) BLADE-ON-PETIOLE genes: Setting boundaries in development and defense. Plant Sci **215**–**216**: 157–171

Khan M, Xu M, Murmu J, Tabb P, Liu Y, Storey K, McKim SM, Douglas CJ, Hepworth SR (2012a) Antagonistic interaction of BLADE-ON-PETIOLE1 and 2 with BREVIPEDICELLUS and PENNYWISE regulates Arabidopsis inflorescence architecture. Plant Physiol **158**: 946–960

Khan M, Tabb P, Hepworth SR (2012b) *BLADE-ON-PETIOLE1* and *2* regulate Arabidopsis inflorescence architecture in conjunction with homeobox genes KNAT6 and ATH1. Plant Signal Behav **7**: 788–792

Khan, M., Ragni, L., Tabb, P., Salasini, B. C., Chatfield, S., Datla, R., et al. (2015) Repression of lateral organ boundary genes by PENNYWISE and POUND-FOOLISH is essential for meristem maintenance and flowering in *Arabidopsis thaliana*. Plant Physiol. **169**, 2166–2186

Kumar S, Mishra RK, Kumar A, Srivastava S, Chaudhary S (2009) Regulation of stipule development by COCHLEATA and STIPULE-REDUCED genes in pea *Pisum sativum*. Planta **230**: 449–458

Kumar S, Sharma V, Chaudhary S, Kumari R, Kumari N, Mishra P (2011) Interaction between *COCHLEATA* and *UNIFOLIATA* genes enables normal flower morphogenesis in the garden pea, *Pisum sativum*. J Genet **90**: 309–314

Li N, Li Y (2014) Ubiquitin-mediated control of seed size in plants. Front Plant Sci **5**: 1–6

Li N, Li Y (2016) Signaling pathways of seed size control in plants. Curr Opin Plant Biol **33**: 23–32

Laguerre G, Mazurier SI, Amarger N. (1992) Plasmid profiles and restriction fragment length polymorphism of *Rhizobium leguminosarum* bv. *viciae* in field populations. FEMS Microbiology Ecology **101**: 17–26

Linkies A, Graeber K, Knight C, Leubner-Metzger G (2010) The evolution of seeds. New Phytol **186**: 817–831

Liu C, Thong Z, Yu H (2009) Coming into bloom: The specification of floral meristems. Development **136**: 3379–3391

Liu S, Magne K, Daniel S, Sibout R, Ratet P (2021) *Brachypodium distachyon* UNICULME4 and LAXATUM-A are redundantly required for development. Plant Physiol **188**(1): 363-381

Magne K, Couzigou J-M, Schiessl K, Liu S, George J, Zhukov V, Sahl L, Boyer F, Iantcheva A, Mysore KS, et al (2018a) MtNODULE ROOT1 and MtNODULE ROOT2 are essential for indeterminate nodule identity. Plant Physiol **178**: 297–316

Magne K, George J, Berbel Tornero A, Broquet B, Madueño F, Andersen SU, Ratet P (2018b) *Lotus japonicus* NOOT-BOP-COCH-LIKE1 is essential for nodule, nectary, leaf and flower development. Plant J **94**: 880–894

Magne K, Liu S, Massot S, Dalmais M, Morin H, Sibout R, Bendahmane A, Ratet P (2020) Roles of BdUNICULME4 and BdLAXATUM-A in the non-domesticated grass Brachypodium distachyon. Plant J **103**: 645–659

McKim SM, Stenvik G-E, Butenko M a., Kristiansen W, Cho SK, Hepworth SR, Aalen RB, Haughn GW (2008) The BLADE-ON-PETIOLE genes are essential for abscission zone formation in Arabidopsis. Development **135**: 1537–1546

Mo X, He L, Liu Y, Wang D, Zhao B and Chen J (2022) The genetic control of the compound leaf patterning in *Medicago truncatula*. Front. Plant Sci. **12**:749989

Norberg M, Holmlund M, Nilsson O (2005) The BLADE ON PETIOLE genes act redundantly to control the growth and development of lateral organs. Development **132**: 2203–2213

Ragni L, Belles-Boix E, Günl M, Pautot V (2008) Interaction of KNAT6 and KNAT2 with BREVIPEDICELLUS and PENNYWISE in Arabidopsis inflorescences. Plant Cell **20**: 888–900

Rodas AL, Roque E, Hamza R, Gomez-Mena C, Minguet EG, Wen J, Mysore KS, Beltran JP and Canas LA (2021) MtSUPERMAN plays a key role in compound inflorescence and flower development in *Medicago truncatula*. Plant J **105**,816–830

Sharma V, Chaudhary S, Kumar A, Kumar S (2012) COCHLEATA controls leaf size and secondary inflorescence architecture via negative regulation of UNIFOLIATA (LEAFY ortholog) gene in garden pea *Pisum sativum*. J Biosci **37**: 1041–1059

Sharma V, Kumar S (2013) Interaction between *cochleata* and *stipule-reduced* mutations results in exstipulate hypertrophied leaves in *Pisum sativum* L. Indian. J Exp Biol **51**: 492–501

Sinjushin AA, Khartina GA, Gostimskii SA (2011) New allele of the COCHLEATA gene in pea *Pisum sativum* L. Russ J Genet **47**: 1422–1427

Sussex IM (1989) Developmental Programming of the Shoot meristem. Cell **56**(2):225-229

Shen D, Xiao TT, van Velzen R, Kulikova O, Gong X, Geurts R, Pawlowski K, Bisseling T. (2020) A homeotic mutation changes legume nodule ontogeny into actinorhizal-type ontogeny. Plant Cell **32**(6):1868-1885

Tavakol E, Okagaki R, Verderio G, Shariati J. V, Hussien A, Bilgic H, Scanlon MJ, Todt NR, Close TJ, Druka A, et al (2015) The Barley Uniculme4 gene encodes a BLADE-ON-

PETIOLE-Like protein that controls tillering and leaf patterning. Plant Physiol **168**: 164–174

Taylor SA, Hofer JMI, Murfet IC, Sollinger JD, Singer SR, Knox MR, Ellis THN (2002) Proliferating inflorescence meristem, a MADS-Box gene that regulates floral meristem identity in pea. Plant Physiol **129**(3): 1150–1159

Toriba T, Tokunaga H, Shiga T, Nie F, Naramoto S, Honda E, Tanaka K, Taji T, Itoh JI, Kyozuka J (2019) BLADE-ON-PETIOLE genes temporally and developmentally regulate the sheath to blade ratio of rice leaves. Nat Commun **10**: 1–13

Wang H, Chen J, Wen J, Tadege M, Li G, Liu Y, Mysore KS, Ratet P, Chen R (2008) Control of compound leaf development by Floricaula/Leafy Ortholog Single Leaflet1 in *Medicago truncatula*. Plant Physiol **146**: 1759–1772

Wang Q, Hasson A, Rossmann S, Theres K (2016) Divide et impera: Boundaries shape the plant body and initiate new meristems. New Phytol **209**: 485–498

Wang Y, Salasini BC, Khan M, Devi B, Bush M, Subramaniam R, Hepworth SR (2019) Clade I TGACG-Motif Binding Basic Leucine Zipper transcription factors mediate BLADE-ON-PETIOLE-dependent regulation of development. Plant Physiol **180(2)**:937-951

Wellensiek SJ (1959) Neutronic mutations in peas. Euphytica **8**: 209–215

Wu X-M, Yu Y, Han L-B, Li C-L, Wang H-Y, Zhong N-Q, Yao Y, Xia G-X (2012) The tobacco BLADE-ON-PETIOLE2 gene mediates differentiation of the corolla abscission zone by controlling longitudinal cell expansion. Plant Physiol **159**: 835–850

Xu C, Park SJ, Van Eck J, Lippman ZB (2016) Control of inflorescence architecture in tomato by BTB/POZ transcriptional regulators. Genes Dev **30**: 2048–2061

Xu M, Hu T, McKim SM, Murmu J, Haughn GW, Hepworth SR (2010) Arabidopsis BLADE-ON-PETIOLE1 and 2 promote floral meristem fate and determinacy in a previously undefined pathway targeting APETALA1 and AGAMOUS-LIKE24. Plant J **63**: 974–989

Yaxley JL, Jablonski W, Reid JB (2001) Leaf and flower development in pea (*Pisum sativum* L.): Mutants *cochleata* and *unifoliata*. Ann Bot **88**: 225–234

Zhang B, Holmlund M, Lorrain S, Norberg M, Bakó L, Fankhauser C, Nilsson O. (2017) BLADE-ON-PETIOLE proteins act in an E3 ubiquitin ligase complex to regulate PHYTOCHROME INTERACTING FACTOR 4 abundance. Elife. 6:e26759

Zhao Y, Liu R, Xu Y, Wang M, Zhang J, Bai M, Han C, Xiang F, Wang ZY, Mysore KS, et al (2019) AGLF provides C-function in floral organ identity through transcriptional

regulation of AGAMOUS in *Medicago truncatula*. Proc Natl Acad Sci U S A **116**: 5176–5181

Zhou C, Han L, Li G, Chai M, Fu C, Cheng X, Wen J, Tang Y, Wang ZY (2014) STM/BP-like KNOXI is uncoupled from ARP in the regulation of compound leaf development in *Medicago truncatula*. Plant Cell **26**: 1464–1479

Zhu B, Li H, Wen J, Mysore KS, Wang X, Pei Y, Niu L, Lin H (2018) Functional specialization of duplicated AGAMOUS homologs in regulating floral organ development of *Medicago truncatula*. Front Plant Sci **9**: 1–14

Zhukov VA, Kuznetsova EV, Ovchinnikova E., Rychagova T., Titov VS, Pinaev AG, Borisov AY, Moffet M, Domoney C, Ellis THN, et al (2007) Gene-based markers of pea linkage group V for mapping genes related to symbioses. Pisum Genet **39**: 19–25

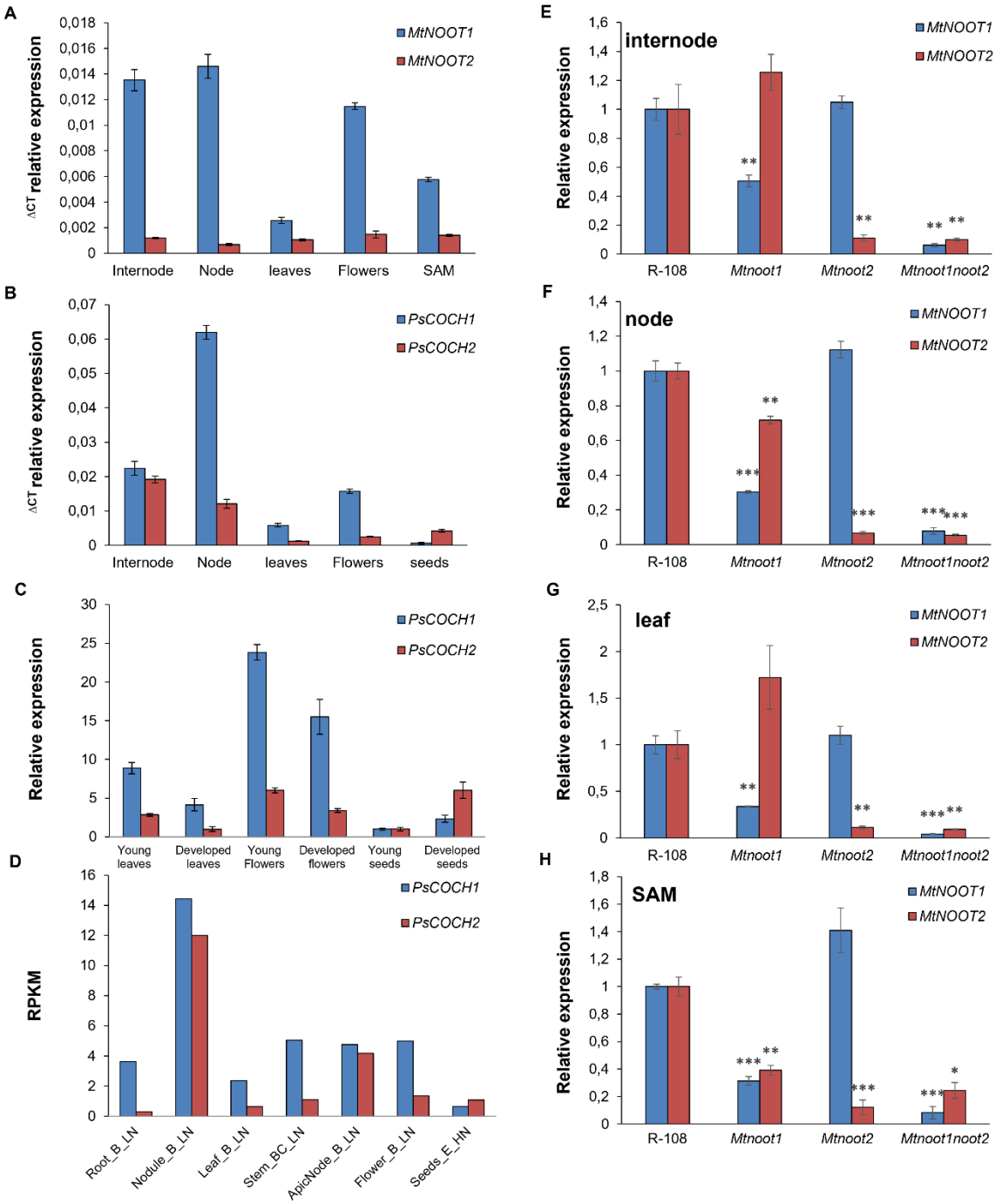

Supplementary Fig. S1. *NBCLs* gene expression patterns in *M. truncatula* and *P. sativum*

A, E-H, *MtNOOT1* (blue bars) and *MtNOOT2* (red bars) RT-qPCR gene expression analysis in (A) *M. truncatula* R-108 internodes, nodes, leaves, flowers and shoot apical meristem (SAM) and in (E-H) *M. truncatula* R-108, *Mtnoot1*, *Mtnoot2*, *Mtnoot1noot2* internodes, nodes, leaves, SAM. (E-H) The low level of expression of the *NBCL* genes in their corresponding mutant backgrounds results from the *Tnt1* insertion nature of the *Mtnoot1* and *Mtnoot2* mutations. *: $p<0.05$; **: $p<0.01$ and ***: $p<0.001$. **B-D**, *PsCOCH1* (blue bars) and

PsCOCH2 (red bars) RT-qPCR gene expression analysis in Caméor internode, node, leaves, flowers and in seeds (B), in young leaves (2 first leaves from shoot apical meristem), in developing leaves, in young flowers (sepal and petal with the same size), in developing flowers (closed flower before aperture), in young seeds (less than 2 mm wide) and in developed seeds (4-5 mm wide) (C) and expression profiles retrieved from the *P. sativum* Gene Expression Atlas (D). For RT-qPCR data, *P. sativum* organs were collected on 35 days old plants, except for developing seeds that were collected from 42-day-old plants. RT-qPCR data represent means ± SEM of three biological replicates. **D**, *PsCOCH1* and *PsCOCH2* gene expression profiles were established using the probe set *Ps*Cam036654 and *Ps*Cam048389, respectively and from the dataset available from the *P. sativum* Gene Expression Atlas. Gene expression data from plants starting to flower (stage B) and grown under low nitrate condition (LN), similar to our growing conditions and stages of development have been retained and organized by organs. RPKM, Reads Per Kilobase Million; stage C, 20 days after the start of flowering; N, grown under nitrate condition; stage E, 12 days after pollination and grown under high nitrate condition (HN).

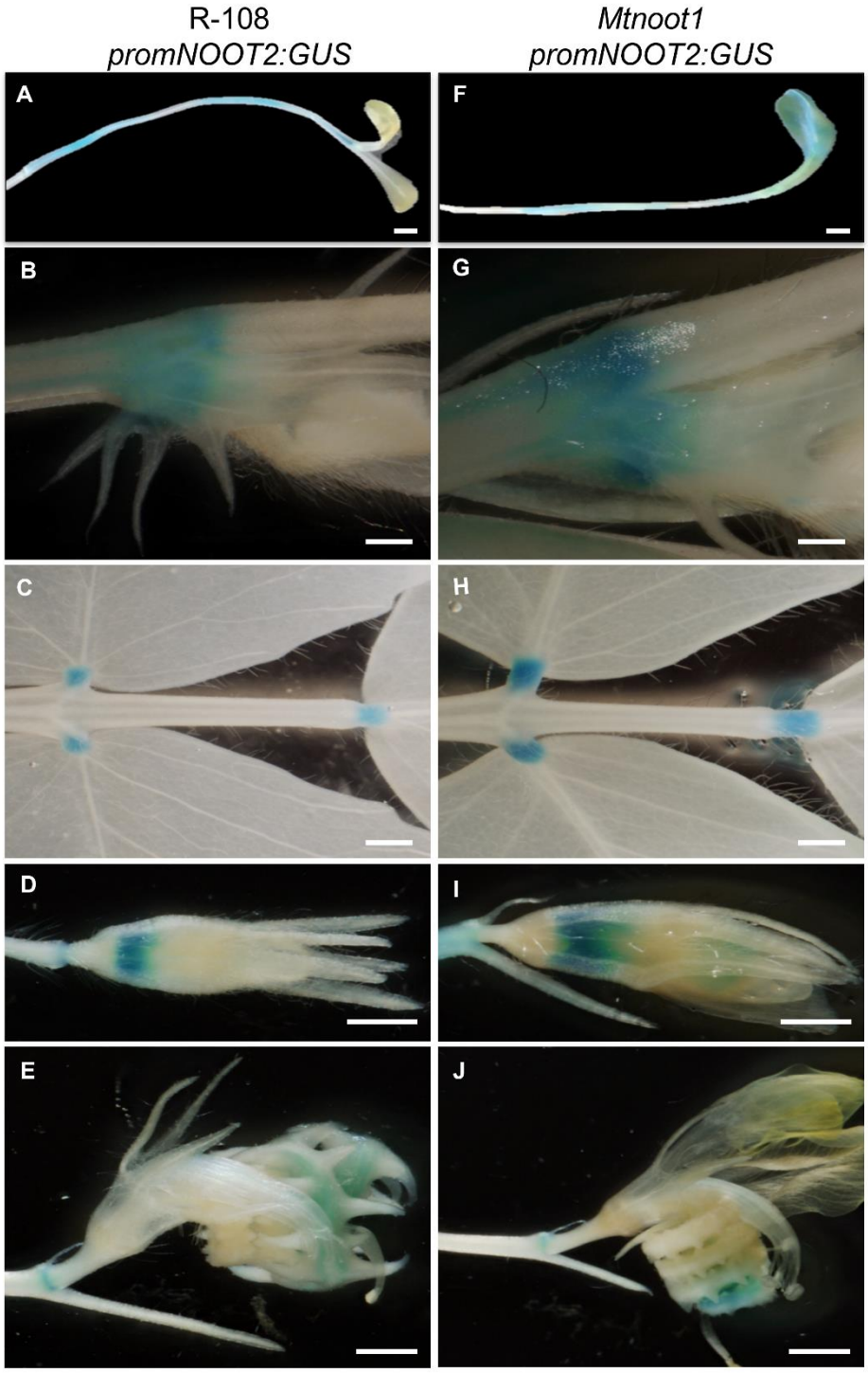

Supplementary Fig. S2. *MtNOOT2* spatial expression in aerial parts of *M. truncatula* R-108 and *Mtnoot1* backgrounds.

A-J, *promNOOT2*::*GUS* gene expression in R-108 (A-E) and in *Mtnoot1* (F-J) backgrounds. The *promNOOT2*::*GUS* gene expression was monitored in young seedling (A, F), at the base of the stipules and petioles (B, G), in leaflet pulvini (C, H), in flower primordia (D, I) and in pods of mature plants (E, J). Scale bars **A-J**: 0.5 cm.

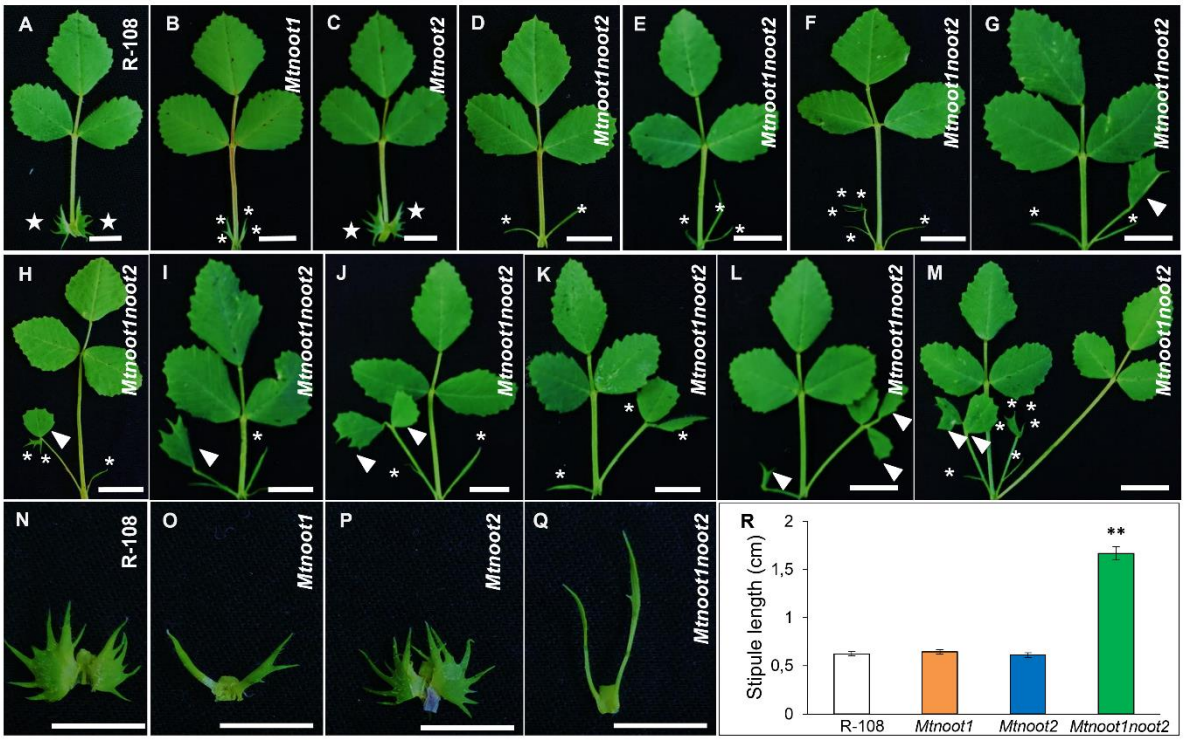

Supplementary Fig. S3. Stipule phenotypes of the *M. truncatula* single and double *nbcl* mutants.

A-M, *M. truncatula* R-108 plants (A), *Mtnoot1* (B), *Mtnoot2* (C) and *Mtnoot1noot2* (D-M). In R-108, a pair of stipules develops at the base of the leaf petiole. R-108 stipules show several serrations above node 3 (A). *Mtnoot1* displays a reduced number stipule serrations (two at each side, B). *Mtnoot2* shows wild-type stipules (C). *Mtnoot1noot2* presents a range of alterations mostly consisting in needle-like structures (D). *Mtnoot1noot2* also presents branched stipules (E-F) or stipule-to-leaf conversions (G-M). **N-Q**, Stipule length in R-108, *Mtnoot1*, *Mtnoot2* and *Mtnoot1noot2*. The length of the stipules is increased in *Mtnoot1noot2* (Q) compared to wild type (N), *Mtnoot1* (O) and *Mtnoot2* (P). Stars indicate wild-type stipules, asterisks indicate needle-like stipules, arrow-heads indicate stipule-to-leaf conversions. Pictures A-D showing *M. truncatula* stipules morphology have also been used in Fig. 3 to illustrate the morphology of leaves. Scale bars **A-Q**: 1 cm. **R**, stipule length measurement in the different *nbcl* mutant backgrounds compared to R-108. **, p-value <0.01.

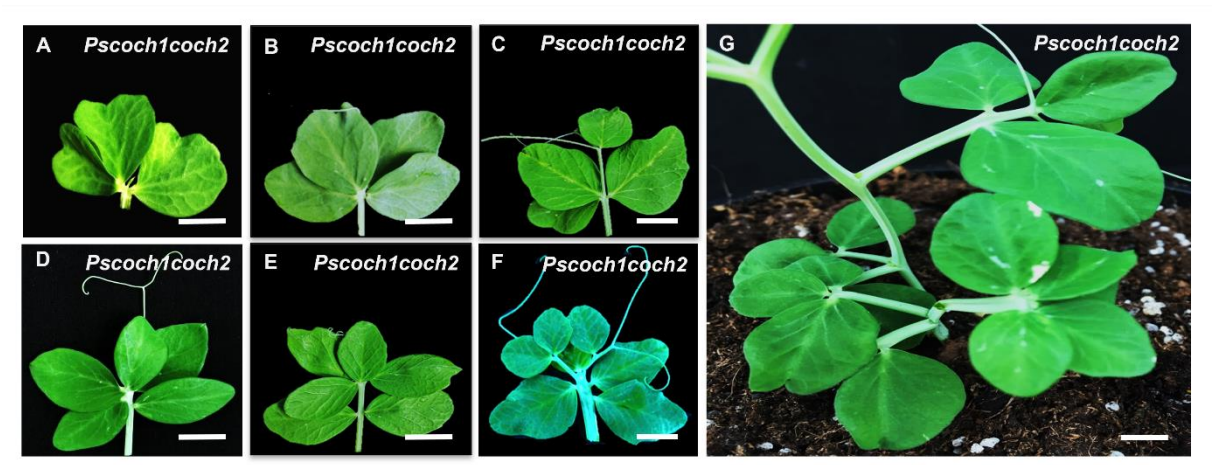

Supplementary Fig. S4. *Pscoch1coch2* leaf phenotypes

A-C, *Pscoch1coch2* leaves with three (A) or four (B) proximal leaflets without terminal tendril. Some leaves occasionally formed a distal leaflet and a terminal tendril (C). **D-F**, *Pscoch1coch2* leaves presenting more than two proximal leaflets (D, G) or forming complex leaves with up to seven leaflets and one or two pairs of terminal tendrils (F).

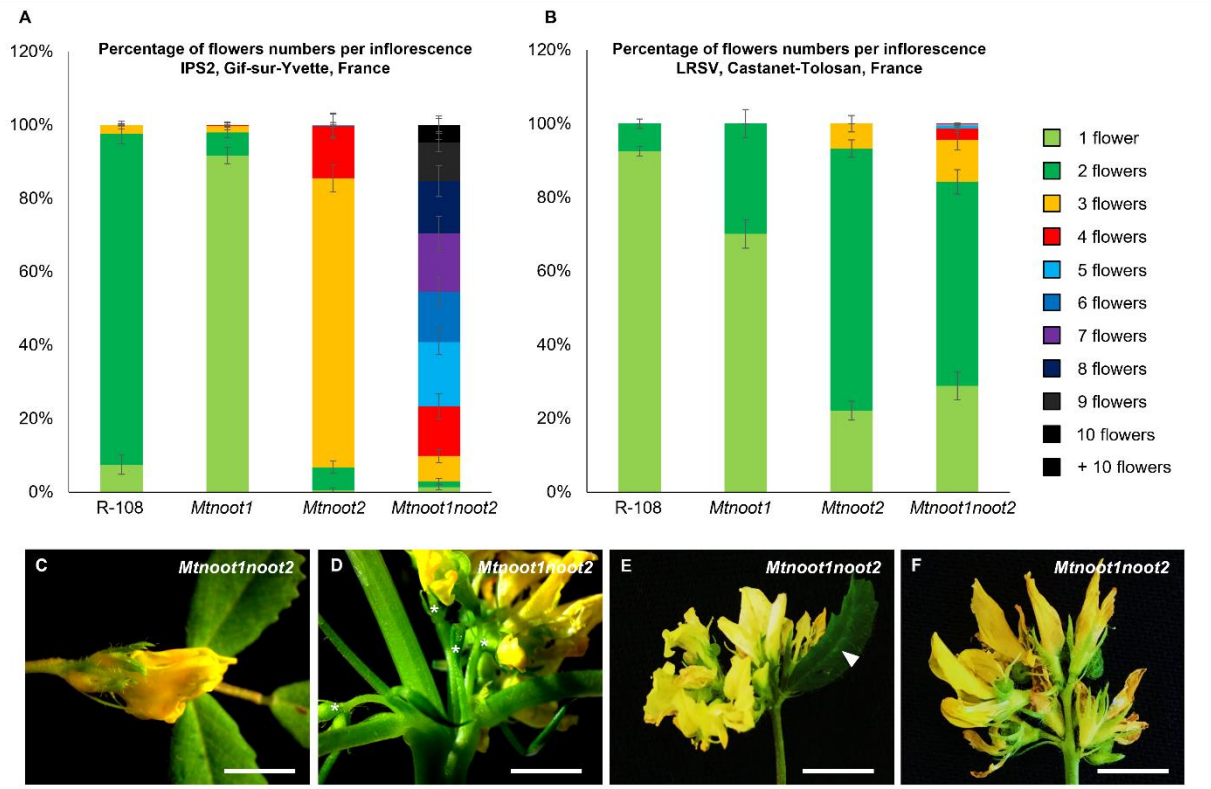

Supplementary Fig. S5. Inflorescence phenotypes in R-108, *Mtnoot1*, *Mtnoot2* and *Mtnoot1noot2*.

A, B, quantification in percentage of the numbers of flowers per inflorescence in R-108, *Mtnoot1*, *Mtnoot2* and *Mtnoot1noot2*. Experiments **A** and **B** have been carried out in two distinct locations, in IPS2, Gif-sur-Yvette, France and in LRSV, Castanet-Tolosan, France, respectively. In R-108 and *Mtnoot1*, mainly one-to-two flowers developed on a single inflorescence. *Mtnoot2* inflorescences carry more flowers per inflorescence than R-108 and *Mtnoot1*. *Mtnoot1noot2* shows an increased number of flowers per inflorescence compared to *Mtnoot2*. In experiment **A**, flower numbers per inflorescence can reach up to 10 or more flowers and in experiment **B**, flower numbers per inflorescence reached up to seven flowers. **C-F**, *Mtnoot1noot2* flowers, lacking pedicel (C) showing multiple inflorescences developing on a single node (D), having an ectopic leaflet (E, white arrow-head) and shortened pedicel (F). **A**, 10 plants and 100 inflorescences per plant were quantified for each genotype. **B**, 27, 22, 27 and 17 plants were analyzed for each genotype, respectively. Scale bars **C-F**: 1 cm.

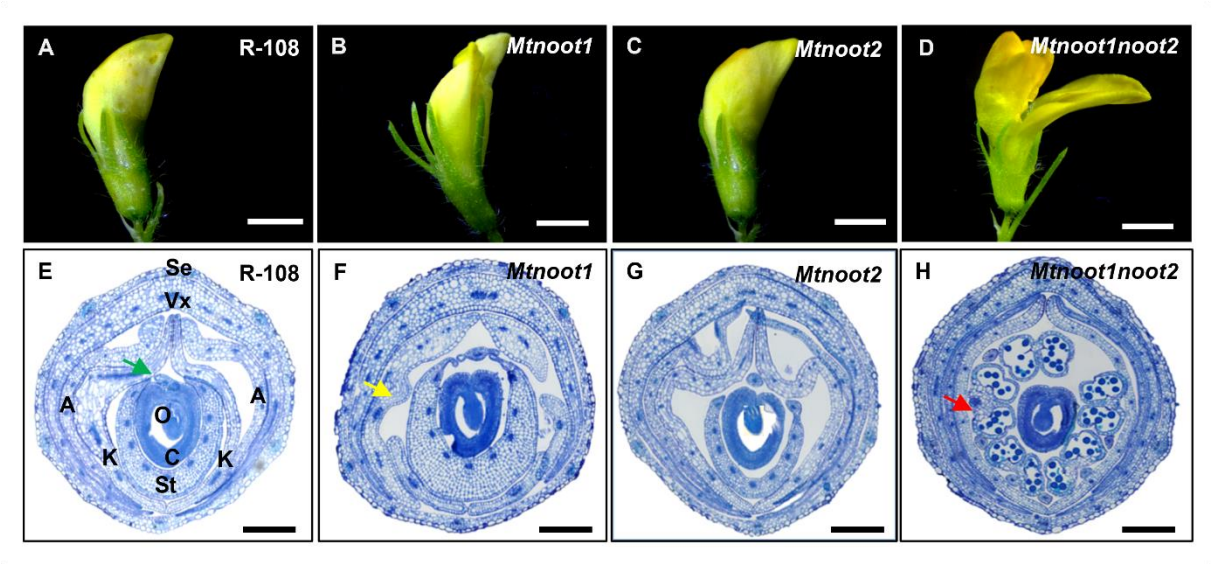

Supplementary Fig. S6. Histological analysis of juvenile flowers of R-108, *Mtnoot1*, *Mtnoot2* and *Mtnoot1noot2*.

A-H, side views (A-D) and transversal sections (E-H) of juvenile flower from R-108 (A, E), *Mtnoot1* (B, F), *Mtnoot2* (C, G) and *Mtnoot1noot2* (D, H). The green arrow points to the stamen filament separated from the fused nine stamens. The yellow arrow points to the extra petal and the red arrow indicates exposed anthers. Se, sepal; Vx, vexillum; A, alae; K, keel; St, staminal tube; C, carpel; O, ovule. Bars: 100 µm.

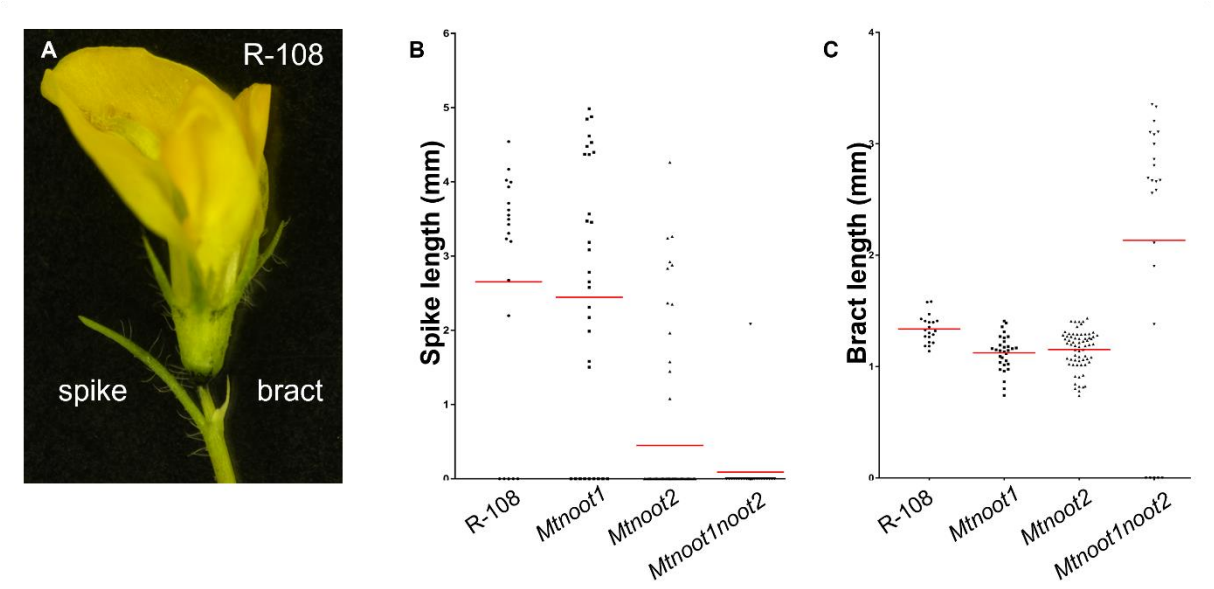

D

	Floral piece fusions (%)		
	Sepal-Petal	Petal-Stamen	Stamen-Carpel
R-108	0,00	0,00	0,00
Mtnoot1	0,00	0,00	0,86
Mtnoot2	0,00	0,00	3,07
Mtnoot1noot2	18,39	45,98	8,05

Supplementary Fig. S7. Spike and bract length, and occurrence of floral organ fusions in the *M. truncatula nbcl* mutants.

A, position of spike and bract on a *M. truncatula* R-108 flower. **B, C,** length of the spike (B) and bract (C) in R-108, *Mtnoot1*, *Mtnoot2* and *Mtnoot1noot2*. **D**, quantification (%) of sepal-petal, petal-stamen and stamen-carpel fusion events in R-108, *Mtnoot1*, *Mtnoot2* and *Mtnoot1noot2*. For R-108, *Mtnoot1*, *Mtnoot2* and *Mtnoot1noot2*, 63, 116, 293 and 87 flowers have been dissected, respectively.

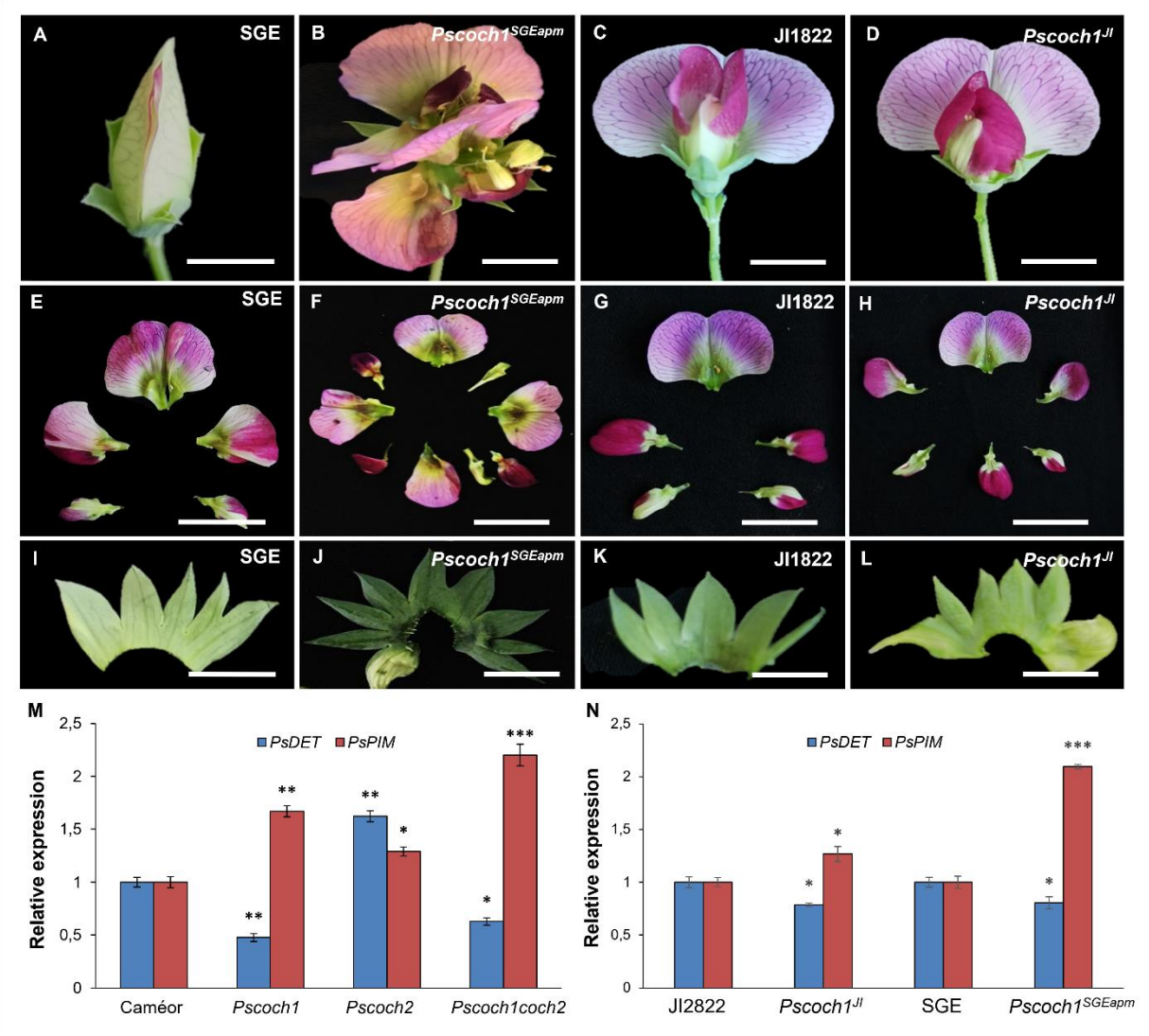

Supplementary Fig. S8. Floral organization in *Pscoch1*^{SGEapm} and *Pscoch1*^{JI} and flower developmental marker genes expression.

A-D, global views of wild type *P. sativum* SGE (A), *Pscoch1*^{SGEapm} (B), wild type JI2822 (C), and *Pscoch1*^{JI} mutant (D) flowers. **E-L,** dissected views of SGE (E, I), *Pscoch1*^{SGEapm} (F, J), JI2822 (G, K) and *Pscoch1*^{JI} (H, L) floral organs. SGE and JI2822 show closed flowers composed by five sepals, five petals. *Pscoch1*^{SGEapm} and *Pscoch1*^{JI} mostly show open flowers with a range of floral patterning defects consisting in an increased petals number, petals identity defects and a loss of floral symmetry (F, H), and an increased sepals number (J, L). Scale bars **A-L**: 1 cm. **M-N**, *PsDET* (blue bars) and *PsPIM* (red bars) RT-qPCR relative gene expression analysis in developed flowers (closed flowers before aperture) from Caméor, *Pscoch1*, *Pscoch2* and *Pscoch1coch2* (M), and in JI2822, SGE, *Pscoch1*^{JI} and *Pscoch1*^{SGEapm} (N). Results represent means ± SEM of three technical replicates and three biological replicates. *, $p<0.05$, **, $p<0.01$ and ***, $p<0.001$.

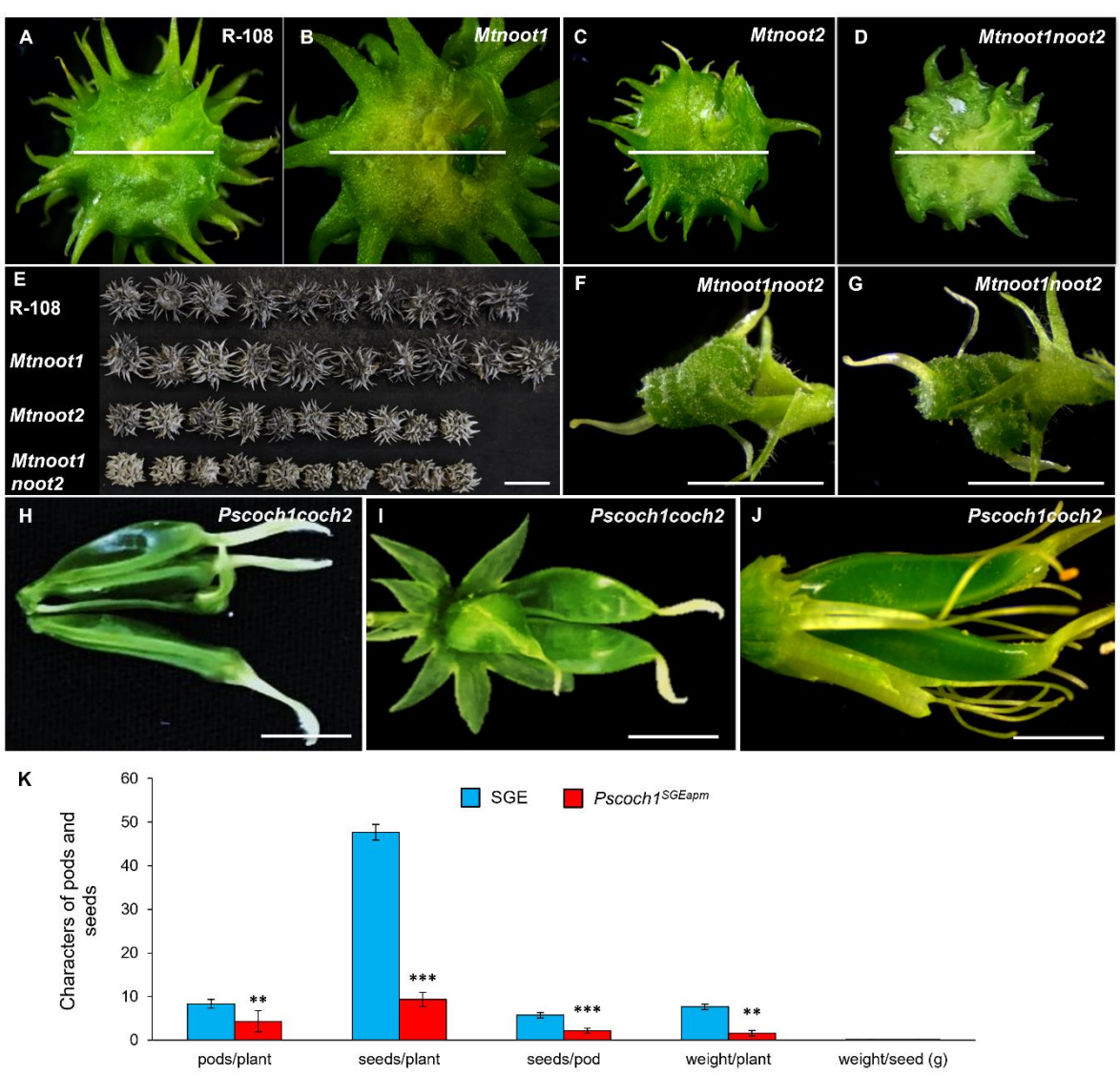

Supplementary Fig. S9. *M. truncatula* and *P. sativum* mutant pods phenotypes.

A-D, young pod sections of R-108 (A), *Mtnoot1* (B), *Mtnoot2* (C), and *Mtnoot1noot2* (D) showing pod diameters. **E**, global views of dried pods of R-108, *Mtnoot1*, *Mtnoot2* and *Mtnoot1noot2*. **F, G**, abnormal *Mtnoot1noot2* pod-like structures. **H-J**, abnormal and fused *Pscoch1coch2* pods. Scale bars **A-D**, **H-J**: 1 cm, **F-G**: 0.5cm. **K,** detailed description of the pod and seed phenotypes in SGE and *Pscoch1*^{SGEapm}. For each genotype, 20 plants were analyzed. **, $p<0.01$ and ***, $p<0.001$.

Supplementary Table S1. Overview of the mutations identified for the *PsCOCHLEATA2* locus by TILLING-NGS

Gene name	Coding sequence size (bp)	Screen coverage (bp)	Screen coverage (%)	Number of families screened	Number of mutants Identified	Knockout mutations	Missense mutations predicted as affecting the protein	Missense mutations predicted as tolerated	Silent mutations
PsCOCHLEATA2	1461	1448	99	4817	75	2	28	27	18

Supplementary Table S2. Mutations identified for the *PsCOCHLEATA2* gene by TILLING-NGS

[a] Position of the mutation in mutants from the starting ATG on the coding sequence. [b] Position of the amino acid substitution in mutants from the starting methionine of the encoded protein. [c] values represent predictive deleterious score from the SIFT software (http://sift.bii.a-star.edu.sg/). SIFT score ranges from 0 to 1. The amino acid substitution is predicted as damaging the protein if the score is ≤ 0,05 (highlighted in blue) and tolerated if the score is > 0,05.

PsCOCHLEATA2			**KX821778**
Nucleic acid transition [a]	Amino acid substitution [b]	SIFT score [c]	Family
C51T	L17L	1	*Ps697*
C51T	L17L	1	*Ps1641*
C51T	L17L	1	*Ps1073*
C100T	R34C	0	*Ps2431*
G106A	V36I	0,36	*Ps4498*
C113T	A38V	0,34	*Ps1865*
C183T	S61S	1	*Ps3370*
G203A	G68E	0,21	*Ps2874*
C233T	P78L	0,34	*Ps3903*
G246A	P82P	0,68	*Ps575*
G268A	V90M	0,03	*Ps1454*
G282A	L94L	1	*Ps4311*
C320T	P107L	1	*Ps2071*
C348T	C116C	1	*Ps3864*
G354A	E118E	1	*Ps2140*
G366A	W122*	0	*Ps1178*
G372A	T124T	0,75	*Ps4616*
C398T	A133V	1	*Ps1527*
G469A	A157T	0,2	*Ps1698*
G507A	M169I	0,43	*Ps3161*
C564T	S188S	0,64	*Ps3495*
C589T	P197S	0,33	*Ps1004*
C594T	P198P	0,49	*Ps3949*
G604A	A202T	0,33	*Ps3693*
G625A	V209I	0,38	*Ps2143*
G645A	E215E	1	*Ps1747*
C662T	S221F	0,04	*Ps737*
C663T	S221S	1	*Ps984*
C670T	R224C	0,02	*Ps3607*
C675T	R225R	1	*Ps3940*
C677T	S226F	0,02	*Ps2078*
C685T	P229S	0,2	*Ps1014*
C690T	L230L	1	*Ps2960*
C690T	L230L	1	*Ps4407*
A695G	H232R	0,69	*Ps4108*
C751T	R251W	0,02	*Ps466*
G753A	R251R	1	*Ps1742*

PsCOCHLEATA2			**KX821778**
Nucleic acid transition [a]	Amino acid substitution [b]	SIFT score [c]	Family
C757T	L253F	0,29	*Ps4235*
C767T	S256L	0,01	*Ps1863*
G792A	M264I	0,05	*Ps1873*
G820A	E274K	0,09	*Ps2220*
C830T	A277V	0,05	*Ps1037*
G841A	A281T	0	*Ps1240*
C935T	P312L	0,08	*Ps2892*
G958A	V320M	0,12	*Ps3451*
G976A	A326T	0,64	*Ps1275*
G1013A	R338K	0,73	*Ps1700*
G1025A	G342D	0,02	*Ps3729*
C1033T	P345S	0,36	*Ps3698*
C1034T	P345L	0,16	*Ps1406*
G1081A	A361T	0,05	*Ps4699*
C1082T	A361V	0,05	*Ps4332*
G1091A	G364E	0,08	*Ps3918*
C1099T	H367Y	0,01	*Ps500*
G1105A	E369K	0,6	*Ps3274*
C1135T	L379F	0,17	*Ps1808*
C1141T	Q381*	0	*Ps3340*
C1165T	R389C	0,03	*Ps3552*
C1188T	N396N	1	*Ps2974*
G1198A	A400T	0,03	*Ps2112*
C1211T	A404V	0,02	*Ps1748*
C1225T	P409S	0	*Ps2701*
C1228T	P410S	0	*Ps4485*
G1240A	D414N	0	*Ps3515*
G1250A	S417N	0	*Ps1414*
G1300A	D434N	1	*Ps1747*
G1312A	V438M	0	*Ps4679*
G1330A	A444T	0	*Ps4168*
C1331T	A444V	0	*Ps1343*
G1346A	G449D	0	*Ps1349*
G1348A	G450S	0	*Ps568*
G1354A	G452S	0	*Ps2270*
G1384A	E462K	0	*Ps3825*
G1403A	G468E	0	*Ps1970*
G1421A	G474E	0	*Ps3335*

Supplementary Table S3. Segregation analysis of the *PsCOCH2 Ps1178* locus

Locus	distribution	wild-type	heterozygous	homozygous	ratio (wt:hetero:homo)
PsCOCH2 Ps1178	theoric	14	27	14	1:2:1
	observed	11	31	12	1:2:1
number of F1 lines: 2; number of F2 plants: 54 ; df: 2; p value: 0.05; X^2: 1,521< critical X^2: 5,99					

Supplementary Table S4. Segregation analysis of double mutants heterozygous for the independent and recessive *PsCOCH1* and the *PsCOCH2* locus

Locus	distribution	*([COCH1COCH2]* and *[COCH1coch2])*	*[coch1COCH2]*	*[coch1coch2]*
PsCOCH1/PsCOCH2	expected ratio	9/16 and 3/16 (12/16)	3/16	1/16
	theoric	120	30	10
	observed	120	29	11
number of F1 lines: 7; number of F2 plants: 160 ; df: 2; p value: 0.05; X^2: 0,133< critical X^2: 5,99				

Supplementary table S5. Oligonucleotides used for TILLING-NGS screen and genotyping

Gene	Gene ID	Family and generation	Forward primer (5'-3')	Reverse primer (5'-3')	Amplicon length
PsCOCHLEATA2	KX821778 KX821779 KX821780 KX821781	*Ps1178* M3, M4	PsCOCH2_Ex1_F2 TTCCCTACACGACGCTCTTCCGATCT ATCTCTCTCCCTTGACTACC	PsCOCH2_Ex1_R1 AGTTCAGACGTGTGCTCTTCCGATCT ACATAAAAACCTGAGTGAGC	498 bp
		-	PsCOCH2_Ex2_1_F1 TTCCCTACACGACGCTCTTCCGATCT TCTTATCTAACTCTCATTGC	PsCOCH2_Ex2_1_R1 AGTTCAGACGTGTGCTCTTCCGATCTT TCCGGAGACACCATCTCGG	615 bp
		-	PsCOCH2_Ex2_2_F3 TTCCCTACACGACGCTCTTCCGATCT CGGCTGGCAAAACTCCGCTT	PsCOCH2_Ex2_2_R1 AGTTCAGACGTGTGCTCTTCCGATCT CTAGCTAGGCTTAGAAATCG	604 bp
			NGS-M13_F CACGACGTTGTAAAACGAC.TTCCCT ACACGAC	NGS-M13_R GGATAACAATTTCACACAGG.AGTTCA GACGTGT	
			M13F700 CACGACGTTGTAAAACGAC	M13R800 GGATAACAATTTCACACAGG	

5' 26 bp illumina adaptators

Supplementary Table S6. Primers used for RTqPCR

Target genes	Primer names	Primer sequences (5' to 3')	Source
PsACTIN	PsACT-F	CTCAGCACCTTCCAGCAGATGTG	Azarakhsh et al. 2015
	PsACT-R	CTTCTTATCCATGGCAACATAGTTC	
PsBETA-TUBULIN3	PsBTUB3_F	TTGGGCGAAAGGACACTATACTG	Saha and Vandemark, 2012
	PsBTUB3_R	CAACATCGAGGACCGAGTCA	
PsCOCHLEATA1	PsCOCH1qpcrD	TCATCCTTATCACGCCGCTC	This study
	PsCOCH1qpcrR	TGCAACTCTCAACCGCGTAA	
PsCOCHLEATA2	PsCOCH2qpcrD	AGACCCCACAGTAAGAACCG	This study
	PsCOCH2qpcrR	TTCACGTGAGAGAACAAGAGC	
PsDETERMINATE (TFL1a)	PsDET-F	CCACCATCAACACCAAACC	This study
	PsDET-R	TCTCTTTCCCAAATGTAGCATC	
PsPROLIFERATING INFLORESCENCE MERISTEM (*PIM*)	PsPIM-4F	GCTTCAGAGTTTGGAACAGC	Liew et al., 2011
	PsPIM-6R	GACTCCATGGTGGTTTGG	
MtACTIN	MtACT-F	TGGCATCACTCAGTACCTTTCAACAG	Plet et al., 2011
	MtACT-R	ACCCAAAGCATCAAATAATAAGTCAACC	
MtRNA RECOGNITION MOTIF	MtRRM-F	AGGGGCAAGTTCCTTCATTT	Plet et al., 2011
	MtRRM-R	GGTAGAAGTGCTGGCTCAGG	
MtNODULE ROOT1	MtNOOT1-F	TATGAATGAAGATCACCACCATAG	Couzigou et al., 2012
	MtNOOT1-R	TCATGACCATGAGAGTGATGATG	
MtNODULE ROOT2	MtNOOT2-F	TTACCCTCCAATGAGCGAAG	Magne et al., 2018a
	MtNOOT2-R	CCAGATCCCTAGGCTTAGAAGTCA	
MtAGAMOUSa	MtAGa-F	TCAAATGACTGCATTACAACCAAG	Zhu et al., 2018
	MtAGa-R	CTAGGAAGCAAATTACAGGTCTTTC	
MtAPETALA1	MtAP1-F	TTGGAGCGCTATGAAAGGTACTC	Zhao et al., 2019
	MtAP1-R	CCCTGTGACTCAGAATCATTTGC	
MtAGAMOUS-LIKE FLOWER	MtAGLF-F	TGAATGGGAAAGAGGTGGTGA	Zhao et al., 2019
	MtAGLF-R	AGAAGCTGGTAACCTATGCAACT	

A Characteristics of the *nbcl* mutant lines used in this study

Mutant names	Abbreviations	Gene accessions	Mutations	Mutant IDs	Mutagens	Backgrounds	References
Mtnodule root1	*Mtnoot1*	Medtr7g090020	*Tnt1* insertion	TNK507	*Tnt1*	R-108	Couzigou et al., 2012
			Tnt1 insertion	NF2717	*Tnt1*	R-108	Couzigou et al., 2012
Mtnodule root2	*Mtnoot2*	Medtr1g051025	*Tnt1* insertion	NF5464	*Tnt1*	R-108	Magne et al., 2018a
Mtnodule root1 nodule root2	*Mtnoot1noot2*	Medtr7g090020 Medtr1g051025	*Tnt1* insertion	NF2717 x NF5464	*Tnt1*	R-108	Magne et al., 2018a
Pscochleata1	*Pscoch1*^{SGEapm}	JN18065	Point mutation R69*	SGEapm	EMS	SGE	Zhukov et al. 2007
	Pscoch1^{JI}	JN180860	Full-length deletion	FN3185/1325	FNB	JI2822	Couzigou et al., 2012
	Pscoch1	JN180861	Full-length deletion	FN3185/1325	FNB	Caméor	This study
Pscochleata2	*Pscoch2*	KX821778	Point mutation W122*	Ps1178	EMS	Caméor	This study
Pscochleata1cochleata2	*Pscoch1coch2*	JN180861 KX821778	Full-length deletion + W122*	FN3185/1325 x Ps1178	FNB/EMS	Caméor	This study

Tnt1, transposon of Nicotiana tabacum 1; EMS, ethyl methanesulfonate; FNB, fast neutron bombardment; *, stop codon

B Schematic representation of the *NBCL* gene structure (top), conserved domains of the corresponding NBCL protein (bottom) and position of the *nbcl* mutations.

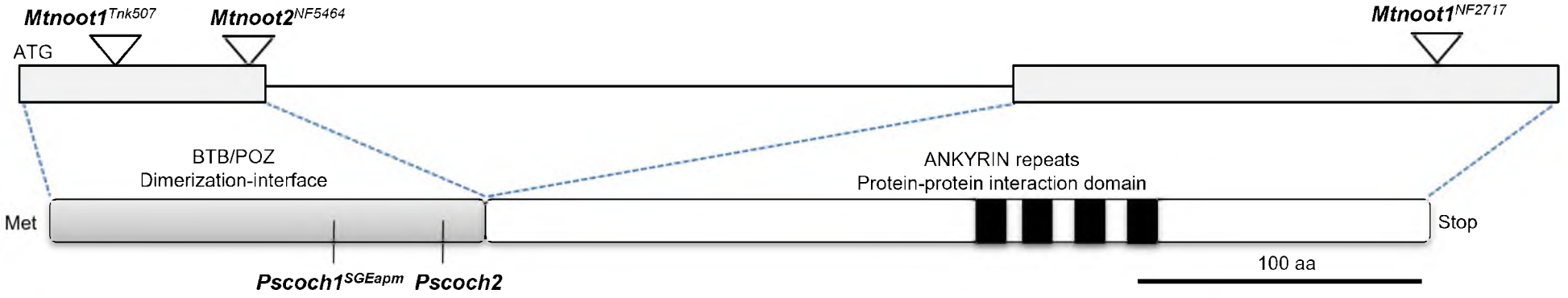

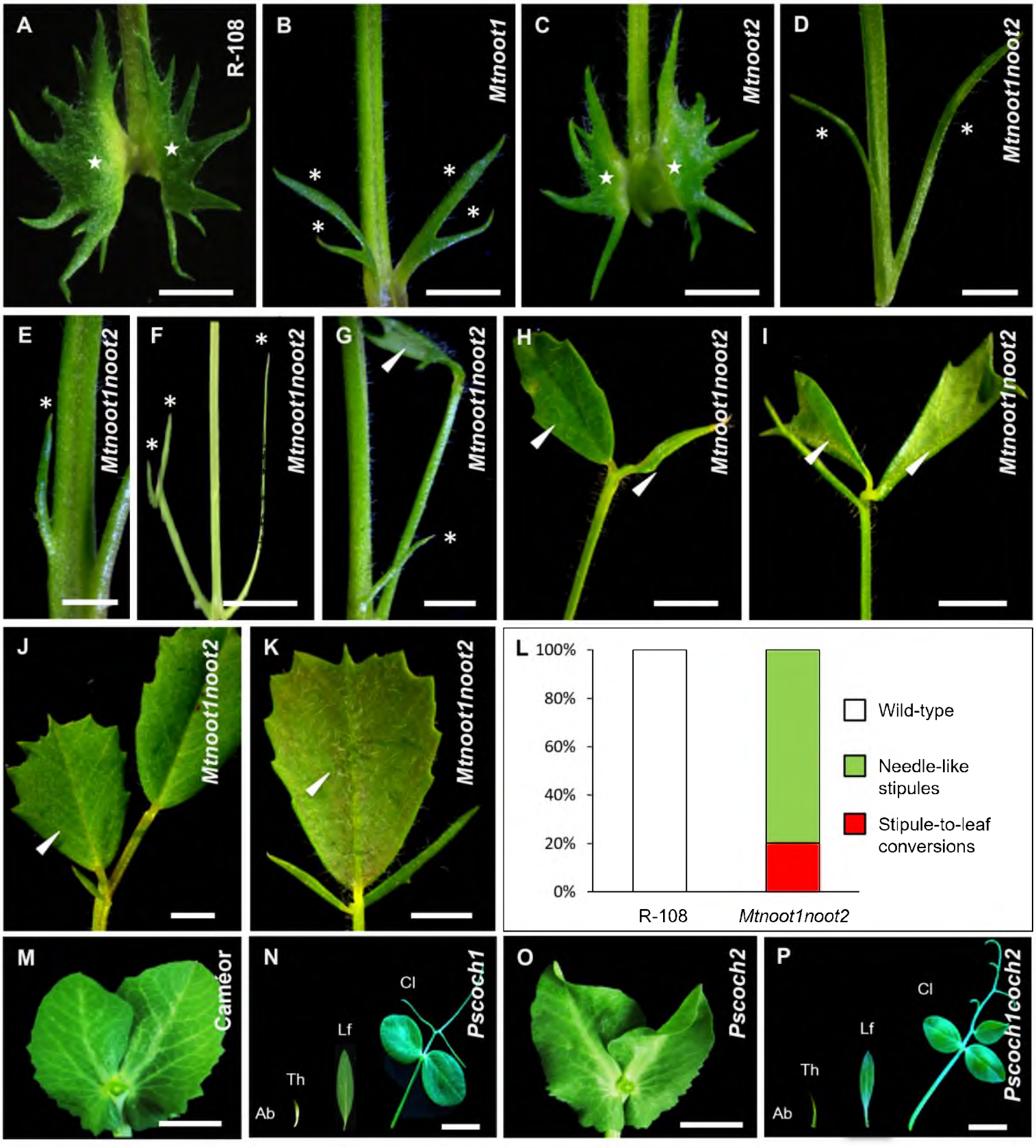

Q

Node position	% Wt	% Lf	% Th	% Ab		% Wt	% Lf	% Th	% Ab		% Wt	% Lf	% Th	% Ab		% Wt	% Lf	% Th	% Ab	
13	100	0	0	0	n: 12	0	100	0	0	n: 6	100	0	0	0	n: 8	0	43	36	21	n: 42
12	100	0	0	0	n: 14	0	83	17	0	n: 6	100	0	0	0	n: 10	0	40	35	25	n: 48
11	100	0	0	0	n: 14	0	80	20	0	n: 10	100	0	0	0	n: 10	0	41	24	35	n: 54
10	100	0	0	0	n: 14	0	60	40	0	n: 10	100	0	0	0	n: 10	0	29	38	34	n: 56
9	100	0	0	0	n: 14	0	67	25	8	n: 12	100	0	0	0	n: 10	0	23	30	46	n: 56
8	100	0	0	0	n: 14	0	57	29	14	n: 14	100	0	0	0	n: 10	0	21	23	55	n: 56
7	100	0	0	0	n: 14	0	43	57	0	n: 14	100	0	0	0	n: 10	0	4	23	73	n: 56
6	100	0	0	0	n: 14	0	29	43	29	n: 14	100	0	0	0	n: 10	0	5	21	73	n: 56
5	100	0	0	0	n: 14	0	7	43	50	n: 14	100	0	0	0	n: 10	0	2	5	93	n: 56
4	100	0	0	0	n: 14	0	14	21	64	n: 14	100	0	0	0	n: 10	0	0	2	98	n: 56
3	100	0	0	0	n: 14	0	14	29	57	n: 14	100	0	0	0	n: 10	0	0	2	98	n: 56
2	100	0	0	0	n: 14	0	0	14	86	n: 14	100	0	0	0	n: 10	0	2	2	96	n: 56
1	100	0	0	0	n: 14	0	0	0	100	n: 14	100	0	0	0	n: 10	0	0	0	100	n: 56
	Caméor					***Pscoch1***					***Pscoch2***					***Pscoch1coch2***				

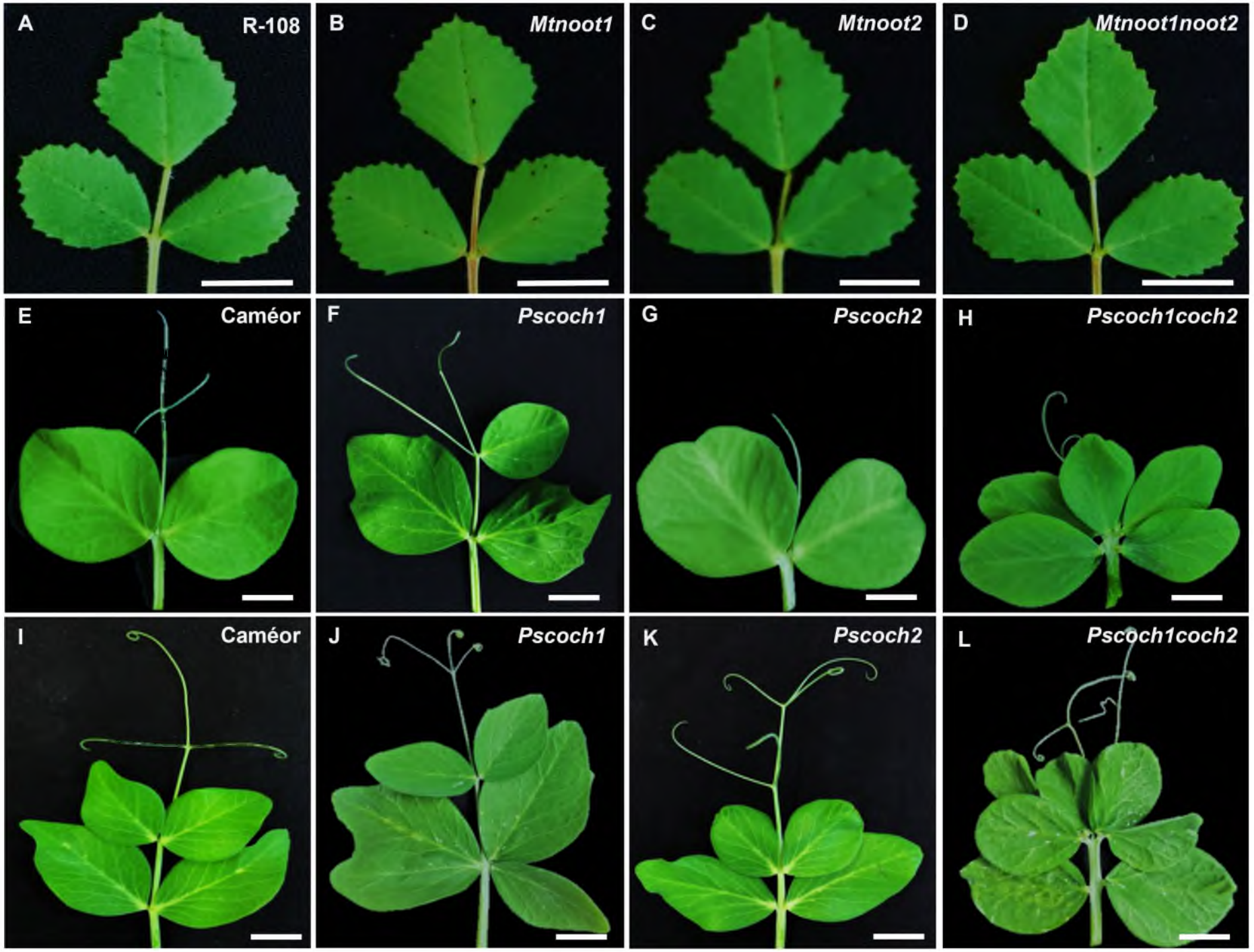
A
R-108
B
Mtnoot1
C
Mtnoot2
D
Mtnoot1noot2
E
Caméor
F
Pscoch1
G
Pscoch2
H
Pscoch1coch2
I
Caméor
J
Pscoch1
K
Pscoch2
L
Pscoch1coch2

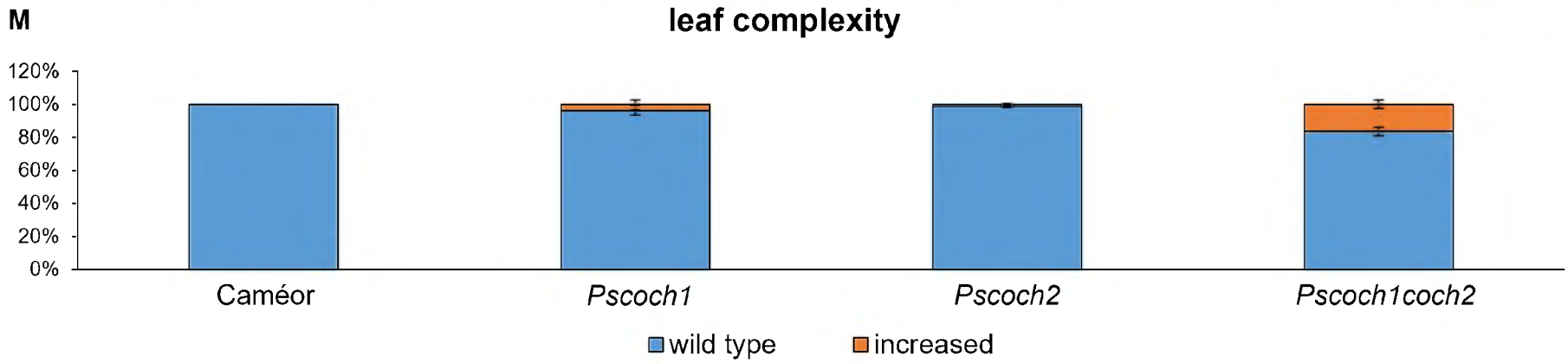
M
leaf complexity
120%
100%
80%
60%
40%
20%
0%
Caméor
Pscoch1
Pscoch2
Pscoch1coch2
wild type
increased

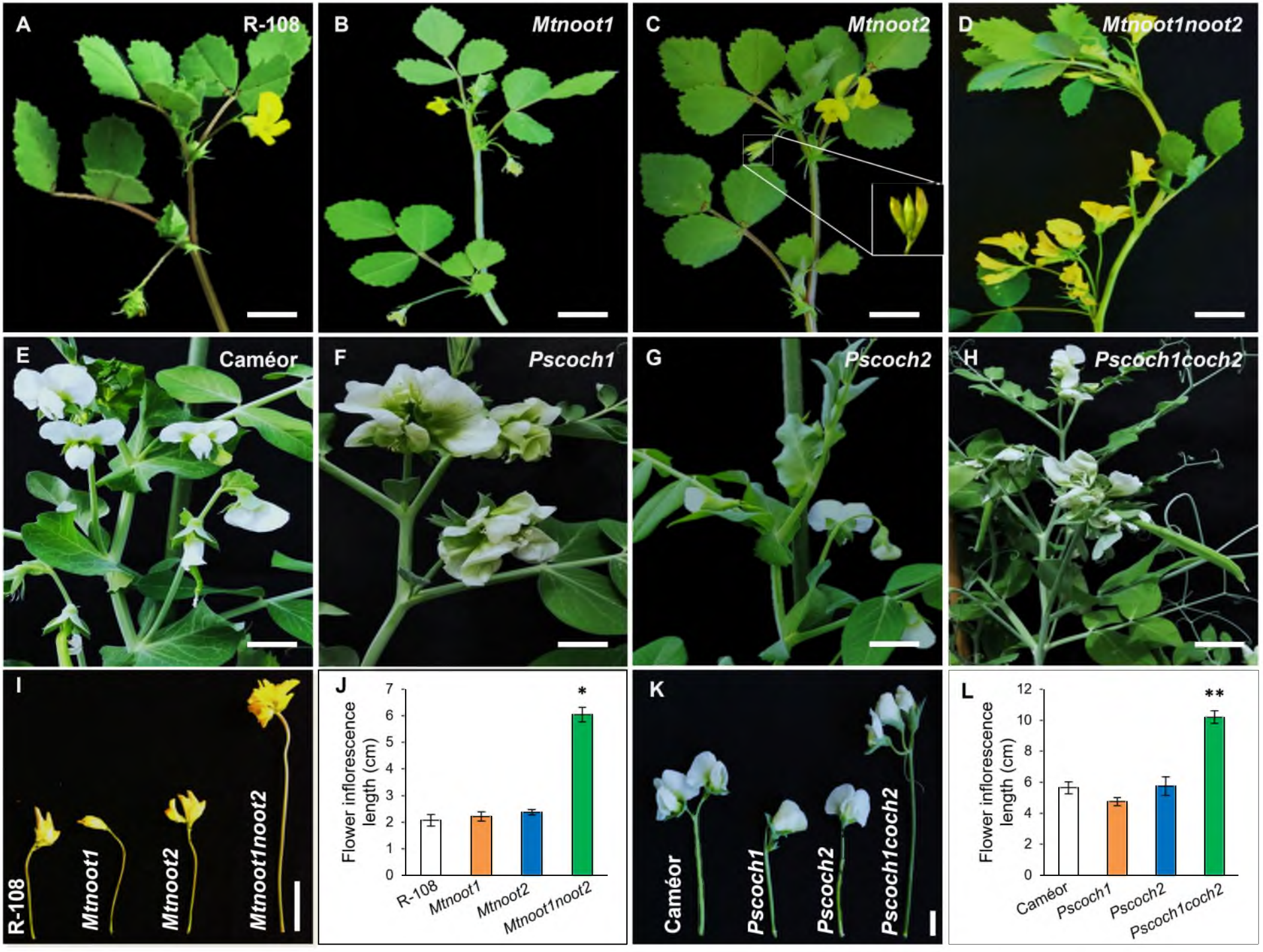
A
R-108
B
Mtnoot1
C
Mtnoot2
D
Mtnoot1noot2
E
Caméor
F
Pscoch1
G
Pscoch2
H
Pscoch1coch2
I
R-108
Mtnoot1
Mtnoot2
Mtnoot1noot2
J
Flower inflorescence length (cm)
0
1
2
3
4
5
6
7
*
R-108
Mtnoot1
Mtnoot2
Mtnoot1noot2
K
Caméor
Pscoch1
Pscoch2
Pscoch1coch2
L
Flower inflorescence length (cm)
0
2
4
6
8
10
12
**
Caméor
Pscoch1
Pscoch2
Pscoch1coch2

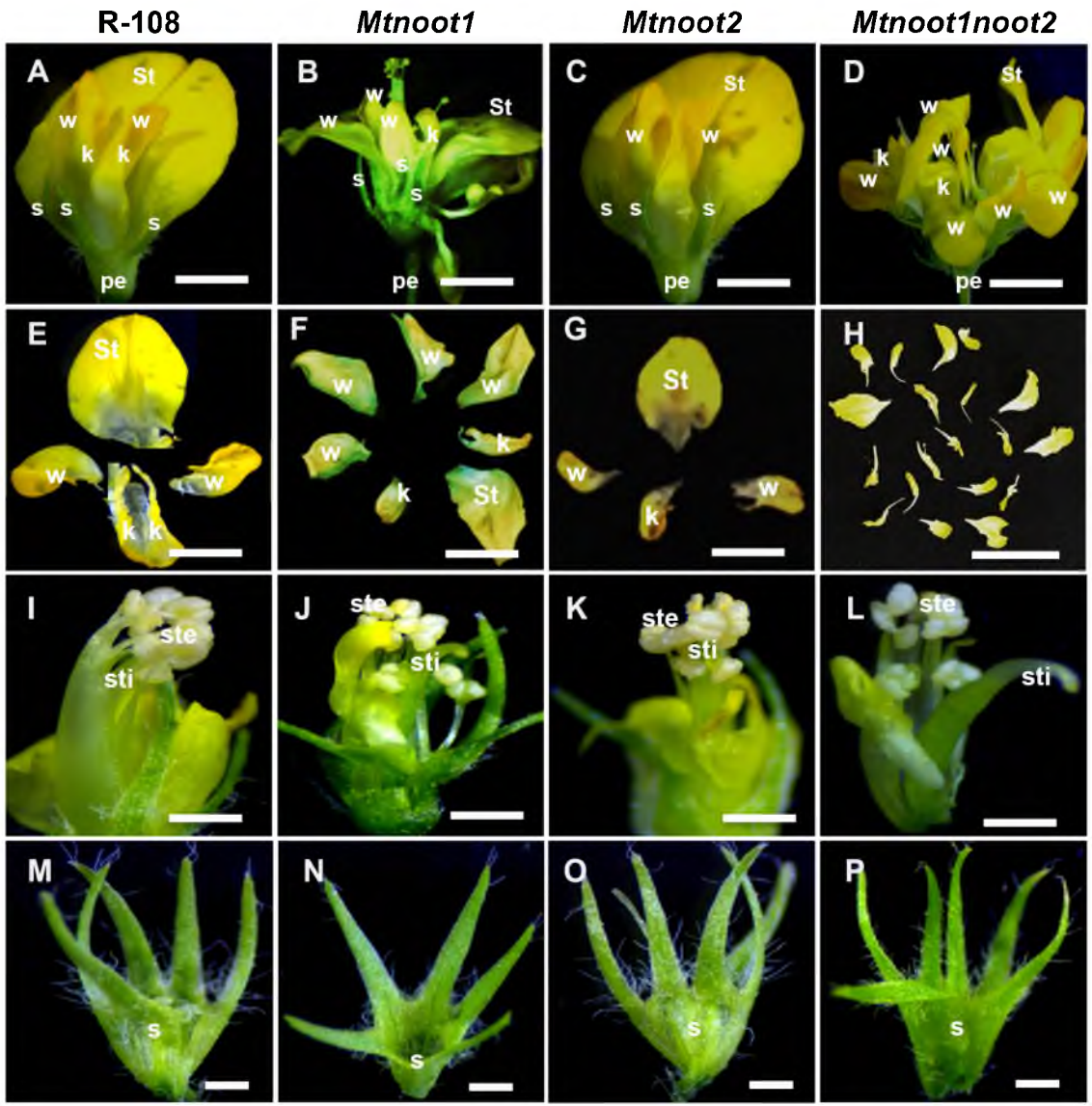
R-108
Mtnoot1
Mtnoot2
Mtnoot1noot2
A
B
C
D
E
F
G
H
I
J
K
L
M
N
O
P
St
w
k
s
pe
ste
sti

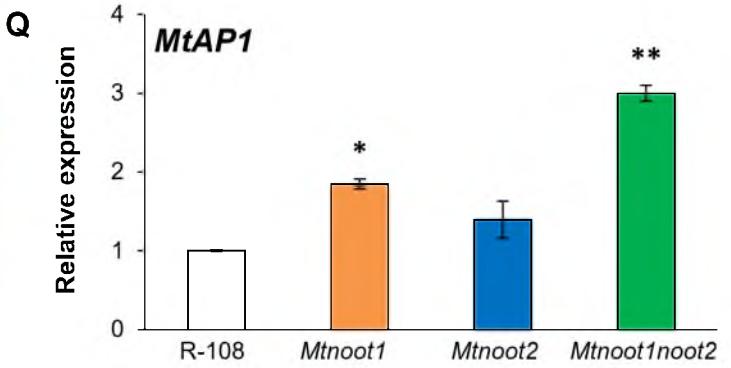
Q
MtAP1
Relative expression
0
1
2
3
4
*
**
R-108
Mtnoot1
Mtnoot2
Mtnoot1noot2

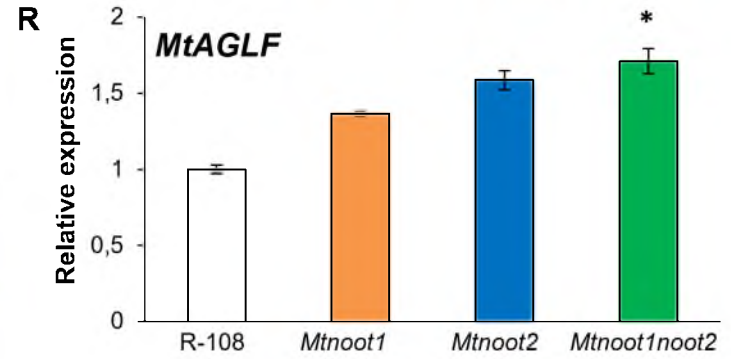
R
MtAGLF
Relative expression
0
0,5
1
1,5
2
*
R-108
Mtnoot1
Mtnoot2
Mtnoot1noot2

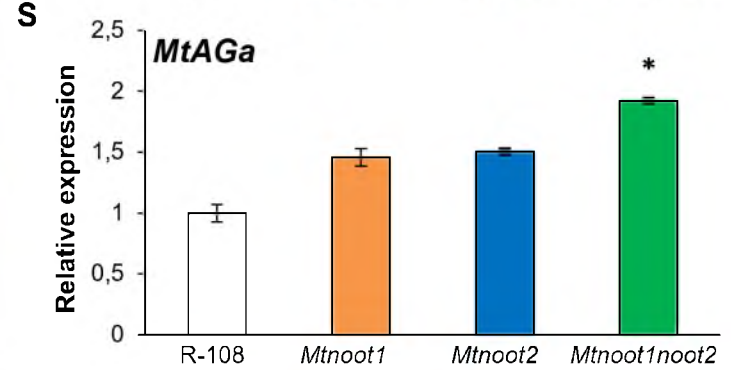
S
MtAGa
Relative expression
0
0,5
1
1,5
2
2,5
*
R-108
Mtnoot1
Mtnoot2
Mtnoot1noot2

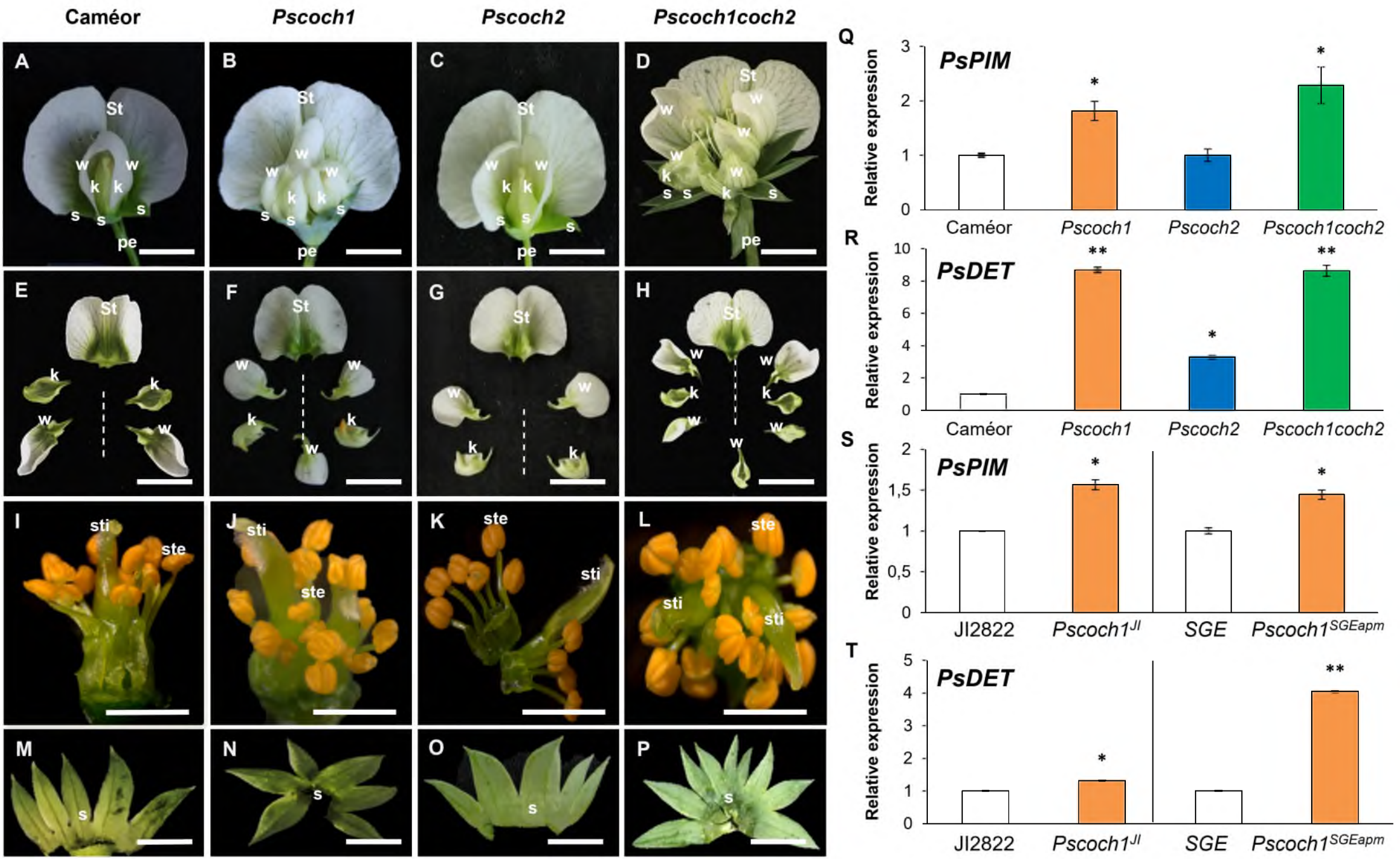
Caméor
Pscoch1
Pscoch2
Pscoch1coch2
A
B
C
D
E
F
G
H
I
J
K
L
M
N
O
P
St
w
k
s
pe
sti
ste
Q
PsPIM
Relative expression
Caméor
Pscoch1
Pscoch2
Pscoch1coch2
R
PsDET
S
PsPIM
JI2822
Pscoch1JI
SGE
Pscoch1SGEapm
T
PsDET

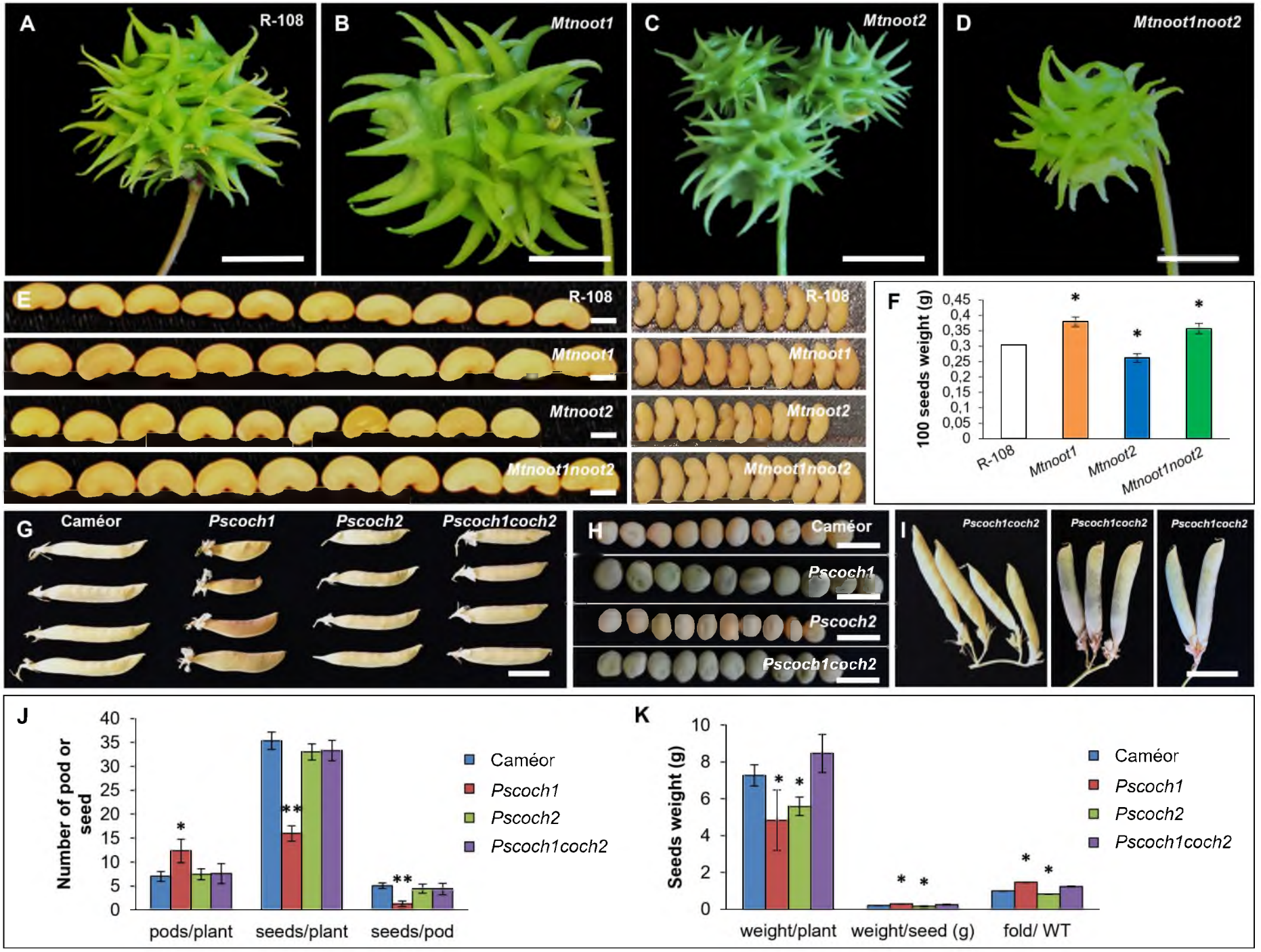
A
R-108
B
Mtnoot1
C
Mtnoot2
D
Mtnoot1noot2
E
R-108
Mtnoot1
Mtnoot2
Mtnoot1noot2
R-108
Mtnoot1
Mtnoot2
Mtnoot1noot2
F
100 seeds weight (g)
0,45
0,4
0,35
0,3
0,25
0,2
0,15
0,1
0,05
0
R-108
Mtnoot1
Mtnoot2
Mtnoot1noot2
G
Caméor
Pscoch1
Pscoch2
Pscoch1coch2
H
Caméor
Pscoch1
Pscoch2
Pscoch1coch2
I
Pscoch1coch2
Pscoch1coch2
Pscoch1coch2
J
Number of pod or seed
40
35
30
25
20
15
10
5
0
pods/plant
seeds/plant
seeds/pod
Caméor
Pscoch1
Pscoch2
Pscoch1coch2
K
Seeds weight (g)
10
8
6
4
2
0
weight/plant
weight/seed (g)
fold/ WT
Caméor
Pscoch1
Pscoch2
Pscoch1coch2

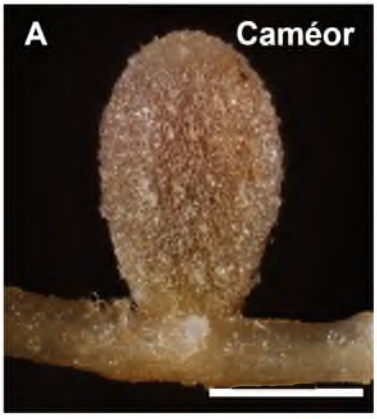
A
Caméor

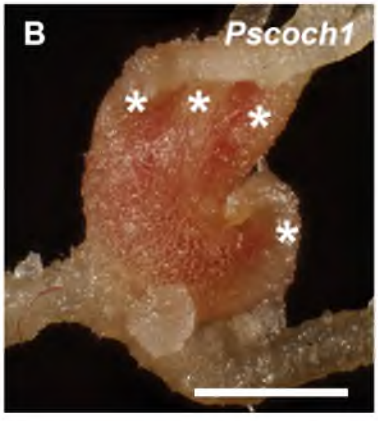
B
Pscoch1

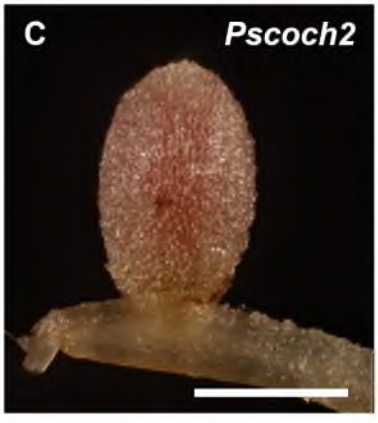
C
Pscoch2

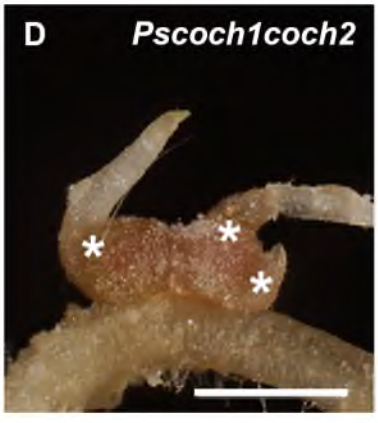
D
Pscoch1coch2

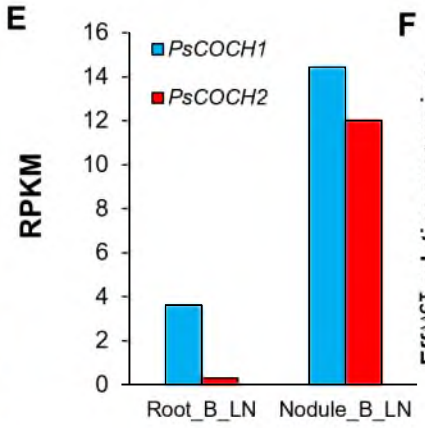
E
RPKM
PsCOCH1
PsCOCH2
Root_B_LN
Nodule_B_LN

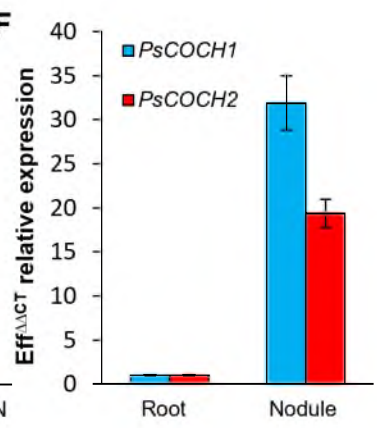
F
Eff^ΔCT relative expression
PsCOCH1
PsCOCH2
Root
Nodule

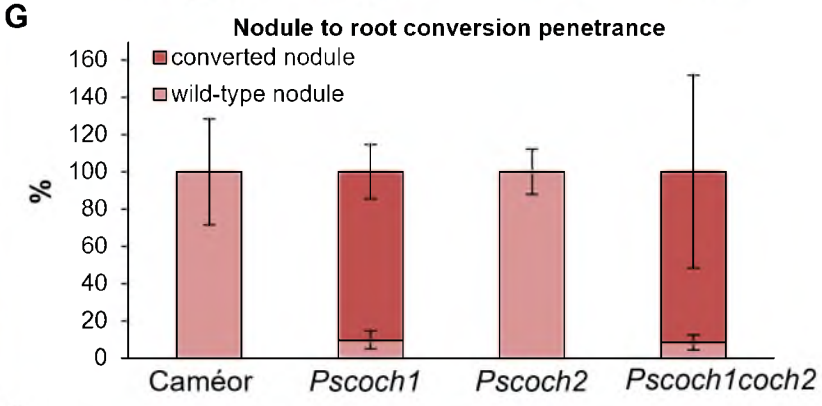
G
Nodule to root conversion penetrance
converted nodule
wild-type nodule
%
Caméor
Pscoch1
Pscoch2
Pscoch1coch2

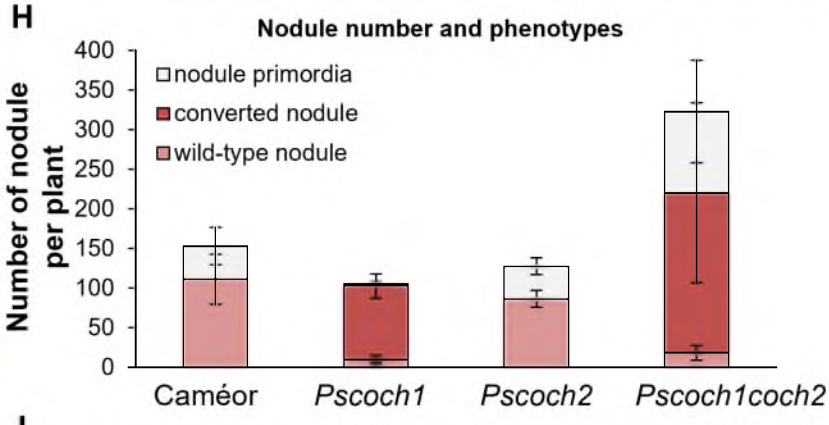
H
Nodule number and phenotypes
nodule primordia
converted nodule
wild-type nodule
Number of nodule per plant
Caméor
Pscoch1
Pscoch2
Pscoch1coch2

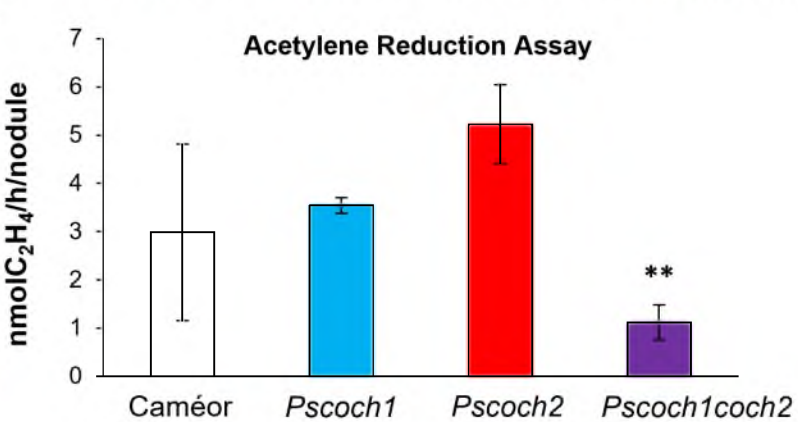
I
Acetylene Reduction Assay
nmolC2H4/h/nodule
**
Caméor
Pscoch1
Pscoch2
Pscoch1coch2